Authors: Rudolph Scherreiks[1], Marcelle Boudagher-Fadel[2]
Affiliations: Geologische Staatssammlung of the Bayerische Staatssammlung für Palaeontologie und Geologie, Germany[1], Professorial Research Fellow, Office of the Vice-Provost (Research), University College London, UK[2]
Orcid ids: 0000-0002-2777-1476[1], 0000-0002-2339-2444[2]
Contact e-mail: m.fadel@ucl.ac.uk

Funder: N/A
DOI: 10.14324/111.444/000078.v3
Preprint first posted online: 14 August 2021
Keywords: Adria, Pelagonia, Vardar, subduction and obduction, ocean lithosphere, tectono-stratigraphy, biostratigraphy, tomographic images, ophiolite, carbonate platforms, The Environment, Climate, Built environment

The closure of the Vardar ocean (the western domain of the northern Neotethys) from early Middle Jurassic to Paleocene time, based on surface geology of eastern Pelagonia and the Vardar zone, biostratigraphy, and seismic-tomographic images of the mantle below the Central Hellenides

Rudolph Scherreiks[1] Marcelle BouDagher-Fadel[2]

[1]Geologische Staatssammlung of the Bayerische Staatssammlung für Palaeontologie und Geologie, Luisenstr. 37, 80333 Munich, Germany
[2]University College London, Office of the Vice-Provost (Research), 2 Taviton Street, WC1H OBT, London, UK

Abstract

Seismic tomographic images of the mantle below the Hellenides indicate that the Vardar ocean probably had a composite width of over 3000 kilometres. From surface geology we know that this ocean was initially located between two passive margins: Pelagonian Adria in the west and Serbo-Macedonian-Eurasia in the east. Pelagonia was covered by a carbonate platform that accumulated, during Late Triassic to Early Cretaceous time, where highly diversified carbonate sedimentary environments evolved and reacted to the adjacent, converging Vardar ocean plate. We conceive that on the east side of the Vardar ocean, a Cretaceous carbonate platform evolved from Aptian to Maastrichtian time in the forearc basin of the Vardar supra-subduction volcanic arc complex.

The closure of the Vardar ocean occurred in one episode of ophiolite obduction and in two episodes of intra-oceanic subduction.

1. During Middle Jurassic time a 1200-kilometre slab of west Vardar lithosphere subducted beneath the supra-subduction, “Eohellenic”, arc, while a 200-kilometre-wide slab obducted onto Pelagonia between Callovian and Valanginian time.

2. During Late Jurassic through Cretaceous time a 1700-kilometre-wide slab subducted beneath the evolving east Vardar-zone arc-complex. Pelagonia, the trailing edge of the subducting east-Vardar ocean slab, crashed and underthrust the Vardar arc complex during Paleocene time and ultimately crashed with Serbo-Macedonia. Since late Early Jurassic time, the Hellenides have moved about 3000 kilometres toward the northeast while the Atlantic Ocean spread.

Key Words Adria, Pelagonia, Vardar, subduction, obduction, tectono-stratigraphy, biostratigraphy, tomographic images, ophiolite, carbonate platforms, ocean lithosphere

Introduction

Relicts of oceanic lithosphere can be traced from the Dinarides through the Hellenides and Taurides. They bear witness to the once extensive northern Neotethys ocean (Fig 1) (Stampfli and Borel 2004; Schmid et al. 2008; Schmid et al. 2020). In this contribution, we shed new light on the paleogeography and subduction of the Vardar branch of the Neotethys from Early Jurassic through Early Paleocene time, which we have gained from our research on the tectono-stratigraphy of the Vardar zone of Greek Macedonia and from the eastern Pelagonian zone of Northern Evvoia and the Northern Sporades (Fig.1). This surface geology is aligned with seismic tomographic images that depict two perturbations in the mantle below the central Hellenides, that we interpret as two slabs of Vardar ocean lithosphere, which sank into the mantle during two episodes of subduction. We also show that two carbonate platforms evolved, one on each side of the Vardar ocean and they reacted to and were tectonically involved with the obduction, subduction and ultimate closure of the Vardar ocean.

A time-lapse reconstruction is presented of the convergence and subduction of the Vardar ocean from Early Jurassic through Early Paleocene time. We give answers to questions concerning the original width of the Vardar ocean and how closure took place and ended with Pelagonia´s collision with the Vardar Island-arc-complex and the detachment and subsidence of the Vardar ocean slabs into the mantle.

Geological Background

The Neotethys, Vardar zone and some nomenclature

In paleogeographic reconstructions of the evolution of the Palaeotethys and Neotethys, Stampfli and Borel (2004) show that the northern Neotethys ocean opened as the Palaeotethys closed (fig. 2a): the Maliac ocean is a remnant of the Paleotethys, which, through intra-oceanic subduction, becomes overthrust by the Vardar ocean at the western end of the northern Neotethys. Alternatively, the Vardar ocean can simply be envisioned to have opened as a western continuation of the Neotethys (Sengor and Natal´in (1996) in Hafkenscheid (2004)).

In an enlightening palaeogeographic reconstruction of the mid-late Jurassic Vardar ocean, shown in Schmid et al. (2020) the Vardar ocean

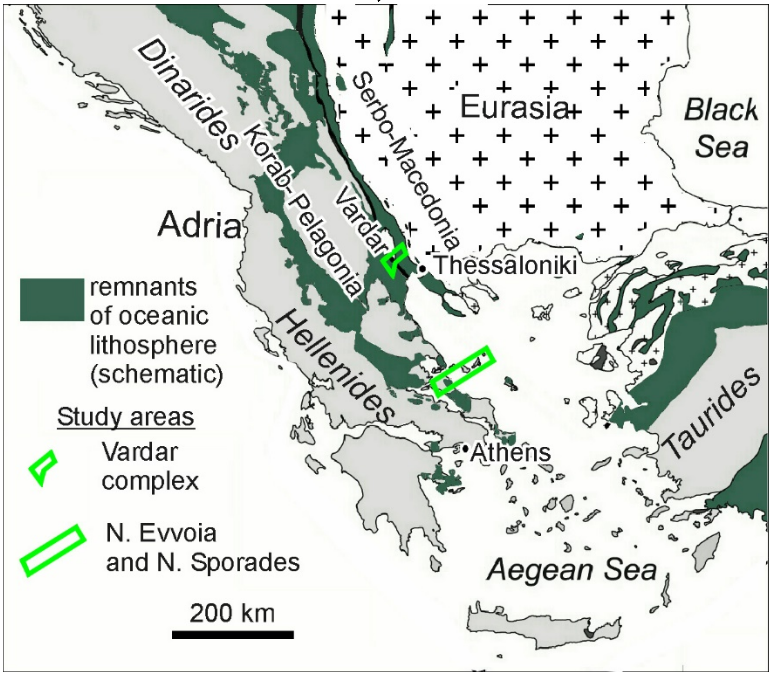

Fig. 1 (see figure captions)

has two eastward dipping, Intra-oceanic subduction zones and an arc complex (Fig.2b). This model implies that the Vardar ocean existed from Early Mesozoic to Late Cretaceous time (in agreement with Sharp and Robertson 2006). Our research corroborates these plate-tectonic paleogeographic interpretations which we have proceeded to investigate both spatially and temporally. Following Schmid et al. (2008) the present contribution supports the one-ocean concept, that the Vardar ophiolites were obducted westward over the Korab-Pelagonian zone of east Adria (Fig. 2b). For other models in which western Pelagonia had plate-tectonic involvement with an inferred Pindos ocean see Sharp and Robertson (2006). Our investigations, however, have been limited to eastern Pelagonia and the Vardar zone (Fig. 1).

Nomenclature

For nomenclatural orientation, “Vardar ocean” is the name of the western ocean domain of the northern Neotethys (Fig.2b). We agree

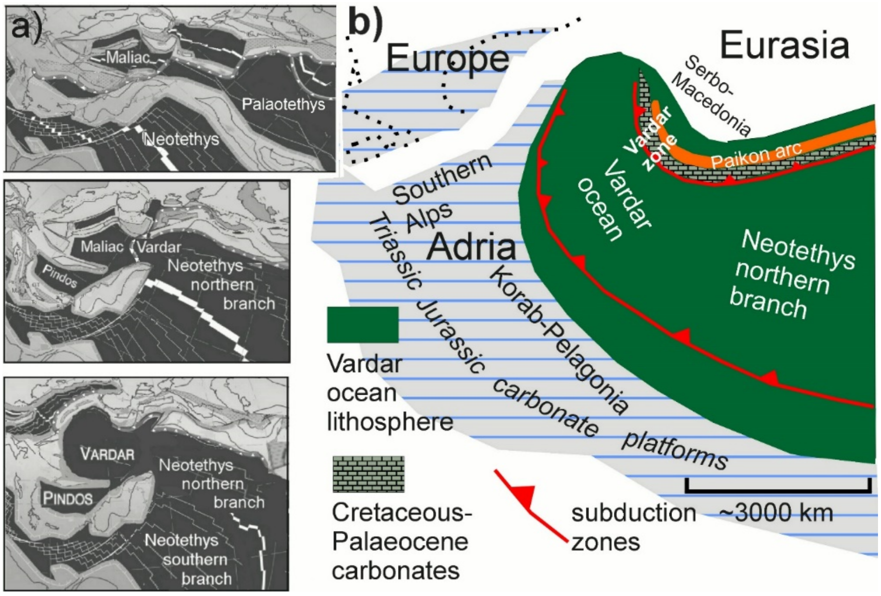

Fig. 2 (see figure captions)

with Schmid et al. (2020) that "Vardar zone" (Fig. 2b) is not synonymous with "Vardar ocean". In our opinion, the Vardar zone is not the "root" "of Vardar-derived thrust sheets, as has been often suggested (Zimmerman and Ross 1976; Brown and Robertson 2004; Froitzheim et al. 2014). Quite the contrary, as will be shown, the "Vardar zone" is where the last slab of the Vardar ocean subducted (Scherreiks and BouDagher-Fadel 2020a and 2020b) and probably corresponds to the "Sava suture zone" (Ustaszewski et al. 2010; Schmid et al. 2020).

The names of geo-tectonic sub-divisions of the Vardar zone used herein are after Kockel (1979).

The "Vardar zone" corresponds to the northwest-southeast striking belt (Fig. 1) where remnants of island arc volcanic formations are found (Mercier, 1968; BeBien et al. 1994; Brown & Robertson 1994; Mercier and Vergely, 2002; Saccani et al. 2008; Sharp and Robertson 2006; Katrivanos 2013) and where easternmost Pelagonia is covered by Upper Cretaceous carbonates (Schmid et al. 2020).

We consider it important to use the term "ophiolite," in the strict sense of the "Steinmann Trinity" (Bernoulli et al. 2003), because there are oceanic formations in the study areas that are composed of basalt +- radiolarite but are devoid of serpentinite and were derived from tectonic environments unrelated to obduction, which will be shown.

Furthermore, the term "mélange", used herein, follows Hsü (1974) referring to tectonically produced polymictic fault-zone rocks as opposed to polymictic sedimentary deposits (see also Scherreiks 2000). The mélanges are associated with mylonitic S-C shear fabrics of subduction zones (Meneghini et al. 2009) like those found in the Vardar zone (Katrivanos et al. 2013).

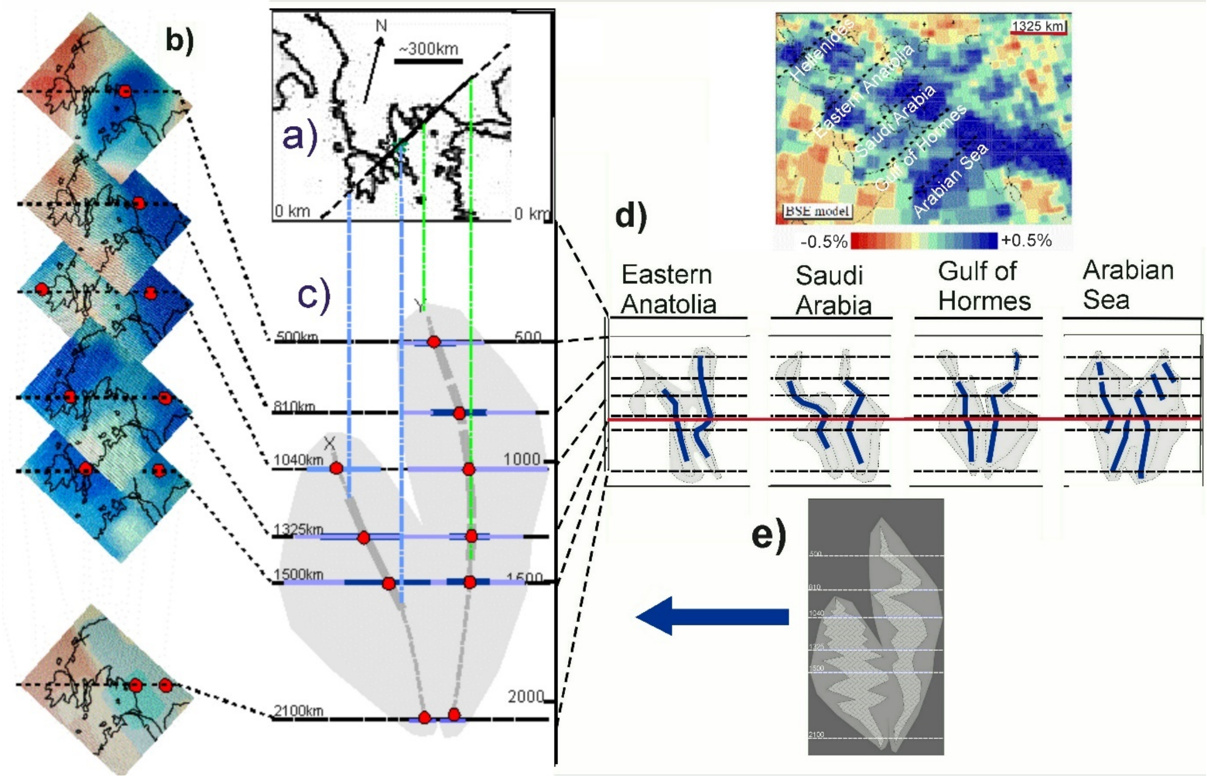

Fig. 3 (see figure captions)

The carbonate platforms of Adria and the Vardar zone

Following the afore said and our own research, Adria was the fundamental pedestal of a vast subsiding carbonate platform, of the <u>marginal, foreland category</u> (Kendall and Schlager 1981; Schlager 2000; Bosence 2005) that extended from the Alps (Fruth and Scherreiks 1982, Bosellini 1984) through Korab-Pelagonia and into the west Taurides (Flügel 1974,1983; Scherreiks 2000) (Fig. 1, Fig. 2b) and across the western Adria (BouDagher-Fadel and Bosence 2007). The platform evolved adjacent to the west side of the Vardar ocean during the Late Triassic through the Early Jurassic from a cyclically alternating supratidal to a peritidal domain (Scherreiks 2000; Bosence et al. 2009) and then responded with subsidence and episodes of upheaval as continental Adria and the Vardar ocean converged (Scherreiks et al. 2010, 2014, 2016). (Table 1a documents biostratigraphic data concerning the Pelagonian carbonate platform of Evvoia and the Northern Sporades, which will be referred to in the text.)

In the Vardar zone at the east side of the Vardar ocean (Fig. 2b) one finds the remnants of a carbonate platform that evolved during the Cretaceous, most probably on the forearc margin of the Vardar arc (Fig.2b) whose evolution terminated during the Paleocene (Mercier 1968; Mercier and Vergely 2002). The inevitable crash between Pelagonia and the Vardar zone (Fig.2b) was a collision between two

Cretaceous platforms (see Discussion). (Significant biostratigraphic data concerning carbonate platform of the Vardar zone are documented in Tables 1b and 1c and will referred to).

The Pelagonian carbonate platform and its involvement in the demise of the Vardar ocean

The Vardar ocean existed during the Middle to Late Triassic, substantiated by radiolarians and pillow basalt found in ophiolite occurrences in our study area in Evvoia (Danelian and Robertson 2001; Chiari and Marcucci 2003; Gingins and Schauner 2005; Gawlick et al. 2008; Scherreiks et al. 2010; Chiari et al. 2012) (Table 1a11.1). Initially, the late Triassic and early Jurassic carbonate platform evolved from a cyclically alternating supratidal to peritidal domain (Scherreiks 2000; Bosence et al. 2009) and then began sinking, presumably responding with subsidence as Adria converged with the Vardar oceanic plate (Scherreiks et al. 2010). The postulated beginning of Intra-oceanic obduction was around Toarcian to Bajocian time (180–170 Ma), based on the ages of amphibolites found in the “metamorphic sole” of subduction-zone mélanges (Roddick et al. 1979; Spray and Roddick 1980; Spray et al. 1984). The platform subsided during the Middle Jurassic, verified by ever deepening carbonate facies (Scherreiks 2000), and then became emergent during Callovian time, verified by bauxite deposits (Fig. 4a) (Scherreiks et al. 2016). The age of this Callovian upheaval has been verified with Bathonian foraminifera in the limestones below, and Oxfordian foraminifera above the bauxite crusts (Table 1a 5 and 6) (ibid.). The “Callovian event” has been attributed to plate tectonic stress that affected the entire Mediterranean region (Meléndez et al. 2007). An Oxfordian transgression re-established shallow marine environments which generated a Tethys-wide reef facies that extended from the Alps to Asia and in the Hellenides is characterised by the

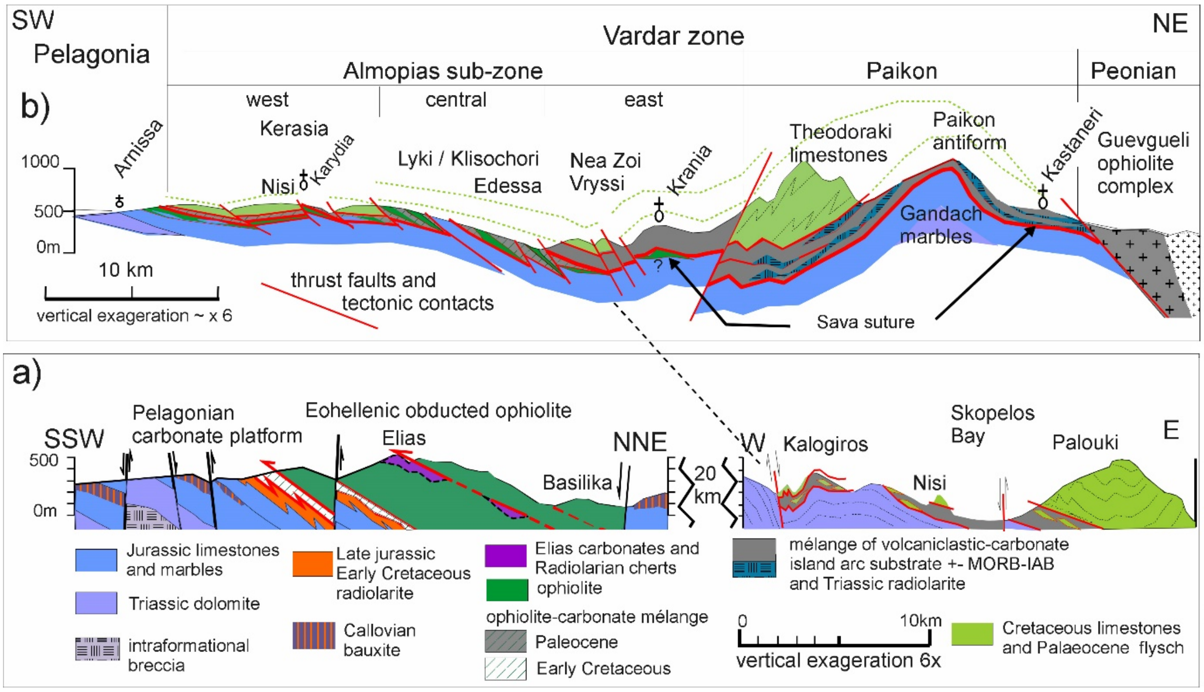

Fig. 4 (see figure captions)

demosponge, *Cladocoropsis mirabilis* Felix (Flügel 1974; Scherreiks 2000) (Table 1a 7 and 8). Rapid platform subsidence and drowning below the CCD occurred during Tithonian-Berriasian time, verified by radiolarian cherts (Baumgartner and Bernoulli, 1976). The final ophiolite emplacement is estimated to have occurred in Valanginian time, in Evvoia, after flysch-like sedimentation had been shut off by the obduction (Scherreiks 2000; Scherreiks et al. 2010; Scherreiks et al. 2014). The obduction was followed by a period of ophiolite erosion (post-Eohellenic unconformity: Scherreiks 2000) and a subsequent gradual, widespread, transgression of marine conglomerate in Evvoia and across the Pelagonian zone during Early Cretaceous time (Fazzuoli et al. 2008; Photiades et al. 2018; Scherreiks 2000) (Table 1a 9).

Paleogeography of the Vardar ocean discerned from seismic tomographic images of the mantle below the Hellenides

Seismic tomographic images of the Alpine-Himalayan realm (BSE models, Bijwaard et al. 1998) depict mantle-perturbations of subducted slabs of Neotethys oceanic lithosphere (Bijwaard and Spakman 2000; Hafkenscheid 2004; van der Meer et al. 2018).

Van Hinsbergen and others (2005) recognised two separate and distinct perturbations in tomographic images as probable Neotethys slabs.

For our investigations, we have enlarged the tomographic images of the areas below the Hellenides and have discerned that there are two slabs: the western slab has a width of about 1200 km, the eastern slab about 1700 km, added together 2900 km (Fig. 3a-c). To check this out, we looked further eastwards to the Arabian Sea (Fig. 3d) and have corroborated that two slabs of oceanic lithosphere have subducted there also. Figure 3d, in detail, is highly interpretive, however, two distinct parallel perturbations are apparent. We have interpreted the perturbations beneath Hellenides as sunken Vardar ocean lithosphere and are of the opinion that the images verify two episodes of subduction (Scherreiks and BouDagher-Fadel 2020a) (Fig. 3c) (see Discussion and conclusions).

The study areas

Evvoia and Northern Sporades

Ophiolites and Platforms

Examples of obducted ophiolite s. str. occur in the study areas of northern Evvoia (Fig. 4a) (Scherreiks 2000; Scherreiks et al. 2014) and are found throughout the Korab-Pelagonian zone (Fig. 1). They lie, tectonically emplaced, together with mélange on top of Upper Jurassic and Lower Cretaceous carbonate platform rocks (Jacobshagen et al. 1976; Jacobshagen 1986). The ophiolites are erosional remnants that have been postulated to be parts of a single obducted ophiolite sheet that was emplaced during the Late Jurassic to Early Cretaceous, an age which classifies it as “Eohellenic” after Jacobshagen et al. (1976). The onetime ophiolite sheet is considered to have had a width of at least 200km - when judged from the width of the ophiolite outcrops on geologic maps (Gawlick et al. 2008; Schmid et al., 2020) (Fig. 1).

The Northern Sporades are devoid of serpentinite. The ophiolite sheet, known to have been obducted over Pelagonia, had been eroded from large areas of Pelagonia during later Lower Cretaceous time (see above). On the Sporades, erosion was extreme; the ophiolite and large parts of the carbonate platform are missing (Fig. 5). The eroded surface of Jurassic and Triassic platform carbonates is covered by a sheet of mélange composed of meta-basalt and radiolarian chert which is chaotically mixed with carbonate breccia and mylonitic phyllonites (Scherreiks and BouDagher-Fadel 2020a) (Fig. 4a and Fig. 5). Slices of Cretaceous and Paleocene platform carbonates of reefal origins are tectonically incorporated in the melange (Table 1a 10-10.3). The Cretaceous carbonate platform successions of Alonnisos and Skopelos overlie the mélange. In corroboration with Kelepertsis (1974) we suggest that the Cretaceous and Paleocene carbonates of the northern Sporades are of Vardar zone origin, which will be expanded upon in the Discussion and Conclusions. The Cretaceous carbonate platform and its mélange substrate, we suggest, correlate with a similar succession in the Almopias sub-zone (Fig. 4a-b).

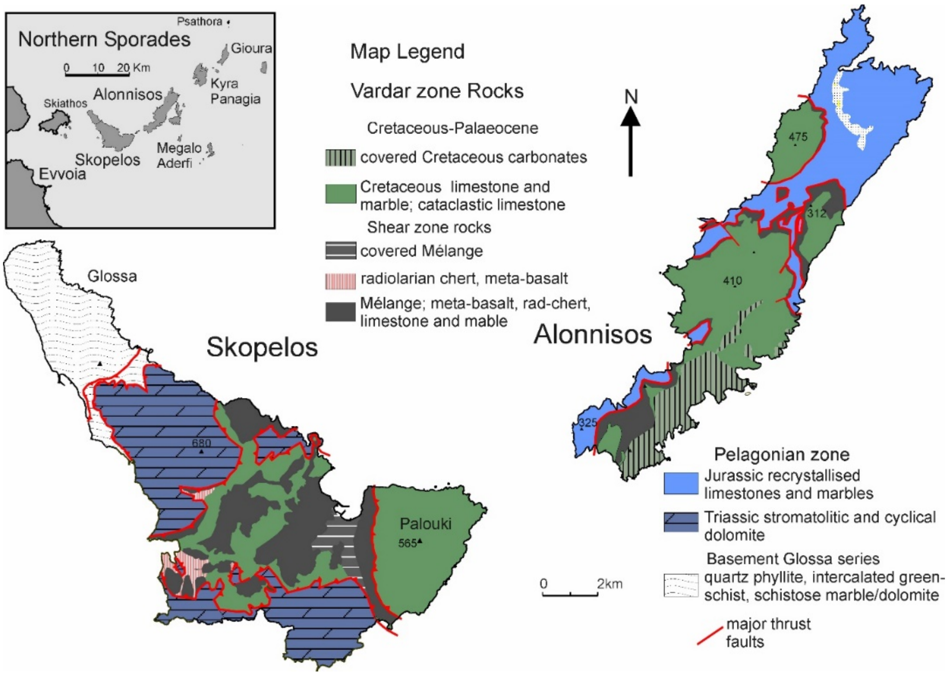

Fig, 5 (see figure captions)

The Vardar zone

West Almopias and its tectonic contact with Pelagonia

Sheared Eohellenic ophiolite occurs on top of Pelagonian carbonates in contact with disrupted Cretaceous limestones (Table 1b 1 and 2), along the western border of the Vardar zone, for example near Panagitsa and Arnissa Fig. 6) (Mercier and Vergely 1988) and southwards near Pygri-Kato Grammatiko and west of the Vermion mountains (Georgiadis et al. 2016) (Fig. 6). West verging imbricated thrust faults characterise this western boundary of the Vardar zone, from the Dinarides through the Hellenides (in Jacobshagen (1986) from Mercier (1973), Mercier and Vergely (1979)). The base of the imbricates is Eohellenic ophiolite and the Triassic-Jurassic carbonate platform of the Pelagonian zone which is covered by disrupted ophiolite followed by schistose pyroclastic units interleaved with slices of radiolarian cherts, volcaniclastic and chloritic marble layers. This tectonic transition between Pelagonia and the western edge of the Vardar zone is shown by Sharp and Robertson (2006) in the Arnissa area (Fig. 6): a ~500-metre-thick succession of imbricated ophiolite mélange. This succession is topped off by limestone debris with rudists and planktonic foraminifera, *Globotruncana* (Mercier and Vergely 1988) (Table 1b 3) (Plate 1). In agreement with these

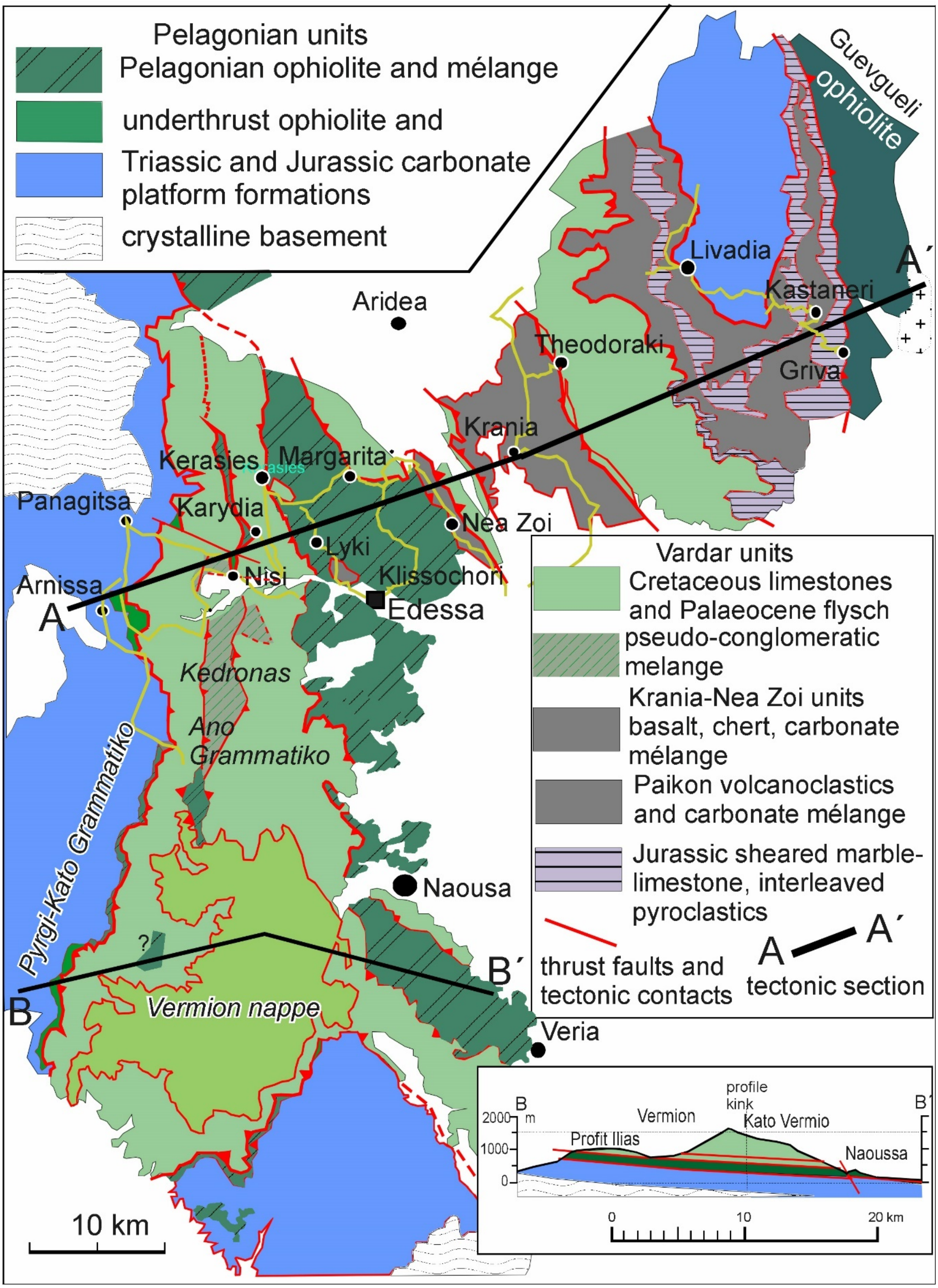

Fig. 6 (see figure captions)

observations, we underscore that the contact between the Vardar and Pelagonian zone is a thrust-fault-zone (see Discussion).
Although Cretaceous carbonates have been supposed to *transgressively* overlie laterite and serpentinite (Mercier and Vergely 1988; Sharp and Robertson 2006; Photiades et al. 2018), we are of the opinion that the inferred transgressional conglomerates are cataclasites (Plate 2a-b) and that orthoconglomerates (Friedman 2003) that could substantiate a marine transgression have not been verified (see Discussion and conclusions). Furthermore, the Cretaceous limestones of the Vardar zone are in tectonic contact with the subjacent allochthonous substrate even where post-Eohellenic laterite is found along the contacts. The circumstances here are similar to the Northern Sporades where a *sedimentary* contact of the Cretaceous Carbonates with their original substrate is nowhere to be found (Scherreiks and BouDagher-Fadel 2020a).

Tectonic windows in west Almopias

Serpentinite and ophiolite-carbonate mélange crop out through the Cretaceous limestone cover in tectonic windows along a narrow, elongated zone of north-south striking faults, extending from Kerassia-Karydia-Kedronas (Mercier and Vergely 1972; 1988) to Ano Grammatiko (Sacciani et al. 2008; Georgiadis et al. 2016) (Fig. 6). Extensive exposures consist of "conglomeratic" rocks (Mercier and Vergely 1988), which in our opinion are cataclasites (see Plate 2 and Discussion). The "conglomeratic" rocks contain Triassic and Jurassic carbonates as well as limestones ranging in age from Cenomanian to Turonian (Table 1b2) and overlie Pelagonian serpentinite (ibid.). Near Nisi and Karydia (Fig. 6) these cataclasites (Plate 2a-b) occur below Campanian limestone (Table 1b 4) (Plate 1). At its base, this succession contains olistolith marbles of Triassic-Jurassic age and overlie white micaceous Triassic marbles in suggested *transgressional* contact (ibid). We dispute a transgressional origin of the Kedronas-Nisi "conglomerate" (see discussion on pseudo-conglomerates). The tectonic windows exposing underthrust Pelagonian ophiolite rocks can be followed in west Almopias from the north near Karydia to the Vermion area (Georgiadis et al., 2016) (Fig. 6, see section B-B´).

Pelagonian ophiolite exposures of central Almopias

An extensive imbricated belt of ophiolite mélange some 50 kilometres long and 5-10 kilometres wide can be traced from the Lyki-Klissochori area (Mercier and Vergely 1984; 1988) to the Naousa and Veria areas (Fig. 6) (Saccani et al. 2008; 2015; Georgiadis et al. 2016). The mélange

is interleaved with slices of marble and Jurassic carbonates, which we agree, are of Korab-Pelagonia origin (Bortolotti et al 2013; Georgiadis et al. 2016) (Table 1b 6 and 7-7.2). The carbonates contain an Oxfordian-Kimmeridgian reefal fauna, including *Cladocoropsis* sp. of Late Jurassic age (Mercier and Vergely 1984). As pointed out above, this is a typical Kimmeridgian-Tithonian reef facies of the Pelagonian zone (Scherreiks 2000) (Table 1a 7-8) that had been overthrust by Eohellenic ophiolite during the Early Cretaceous. In the Vardar zone, the Pelagonian ophiolites are locally interleaved with sericitized basalt schist (Lyki) (see Geochemistry) and are underthrust position beneath “conglomeratic”, ophiolitic mélange and upper Cretaceous carbonates (east of Margarita, Fig. 6) (Table 1b 7).
In accord with the afore cited researchers and the described geology, we support the opinion that the ophiolites and upper Jurassic carbonates found in the west and central Vardar sub-zones are tectonically inherited from the underthrust Pelagonian plate (Fig. 4b).

Eastern Almopias and Paikon units

A noteworthy difference between the eastern and western units of the Vardar zone is that the eastern Almopias and the Paikon units appear to be devoid of serpentinite which we corroborate from Tranos et al., 2007. Serpentinite, however, probably exists at depth (Fig. 4b), because further north in an area known as Ano Garefi serpentinized peridotite is exposed below basalt (saccani et al. 2015). The mélanges of the Nea zoi-Vryssi-Meglenitsa and Krania units (Fig. 4b and Fig. 6) are composed of dolerite, pillow basalt and tuff and contain upper Jurassic-lower Cretaceous radiolarite (Mercier and Vergely 1984), with a relict Cretaceous cover (Table 1c 1.-1.2). Slices of Triassic lavas and radiolarites (Stais et al. 1990) (Table 1c 3 and 4) and upper Cretaceous arenites are also incorporated into the foliated matrix of the mélange of the Krania-Vryssi units (Saccani et al. 2015). The “*ophiolite related”* mafic units, *“ophiolite nappe”* and *“Meglenitsa Ophiolite*”, reported in Sharp and Robertson 2006 (from Sharp and Robertson 1994 and Sharp & Robertson 1998), in our opinion are not ophiolites s. str. but consist of ocean floor or arc basaltic rocks (see Geochemistry).

The Paikon antiform, a Pelagonian window: Katrivanos et al. 2013

The Theodoraki limestone is the youngest formation of the Paikon antiform (Katrivanos et al. 2013). This limestone is part of the Cretaceous carbonate platform that covers the entire Vardar zone, and is composed of a wide range of neritic to reefal facies (Table 1b and Table 1c Theodoraki unit). The platform is in tectonic contact with a pile-up of SW dipping slices of Theodoraki limestones and slices of volcano-

sedimentary rocks including radiolarites, tuffites and lava, and Triassic-Jurassic Marble and schist of Pelagonian origin (Mercier and Vergely 2002). Katrivanos and others (2013) corroborate that the tectono-stratigraphic sequence is composed of volcano-clastic rocks together with limestones of Middle to Late Jurassic age, based on micro and macro-faunas including *Cladocoropsis mirabilis* (Griva-Kastaneri formation Fig. 4b, Fig. 6) (Table 1c Griva-Khromni units). The volcano-sedimentary slices are on top of Triassic-Jurassic Gandatch marbles and schists (Fig. 6). All the volcanic material of this series is *strongly mylonitized in discrete, narrow shear zones* related to mylonitic foliation (Katrivanos et al. 2013). The carbonate rocks are mylonitized, near the contacts with tectonically overlying volcano-sedimentary slices e.g., at Kastaneri (ibid). Our investigations corroborate the above observations, which lead us to interpret the volcano-sedimentary formations in the substrate of the Theodoraki limestone as a composite allochthonous mélange complex in which slices of volcanic and sedimentary rock-units can be individually distinguished.
In contrast to the above, the Paikon unit has been depicted (Sharp and Robertson 1994) to consist of a contiguous sedimentary, stratigraphic, succession extending from the Triassic to Cretaceous time only interrupted by two unconformities, an Oxfordian and a Cenomanian.

We share the opinion that the Paikon is an antiform and a Pelagonian tectonic window (Katrivanos et al. 2013), and that the Paikon unit of the Vardar zone was most probably part of a volcanic island arc complex (Mercier et al. 1975; Mercier et al. 2002; BeBien et al. 1994; Brown & Robertson 2004; Mercier and Vergely 2002; Saccani et al. 2015, Schmid et al. 2020). Our mutually envisioned island arc scenario evolved as the eastern Vardar ocean subducted north-eastwards towards the margin of the European continent, which initiated supra-subduction arc volcanism (Mercier and Vergely 2002; Brown and Robertson, 2004; Saccani et al., 2015). This was accompanied by back-arc spreading (Hafkenscheid, 2004; Schmid et al. 2020), represented by the Guevgueli ophiolite complex (Fig. 4b) (Anders et al. 2005; Saccanni et al. 2008b; Bortolotti et al. 2013; Michail et al. 2016).

Geochemistry
Meta-basalts from the Vardar zone and from northern Evvoia have been analysed for their major, minor and trace element contents, and some previous analyses are shown from the Northern Sporades (Scherreiks and BouDagher-Fadel 2020a). The analytical results are in Tables 2a

and 2b. Rare-Earth (REE) plots and ternary discrimination diagrams (Fig. 7) have been drafted for the purpose of ascertaining basalt origins (after Pearce and Cann 1973; Perfit et al.1980; Vermeesch P, 2006).

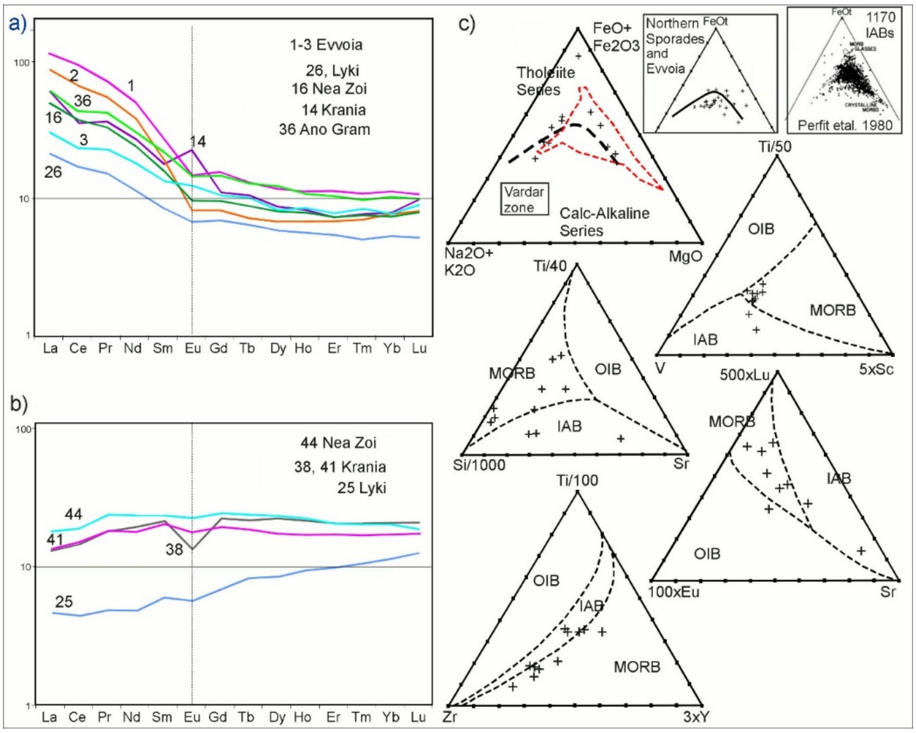

Fig. 7 (see figure captions)

Two serpentinized peridotites associated with basalts and radiolarian cherts from Pelagonian ophiolites of Evvoia were previously analysed (Scherreiks and BouDagher-Fadel 2020a) (Table 2b).
The meta-basalts of the Vardar zone and the Northern Sporades occur in mélanges and they are sheared and sericitized and strongly weathered, which may have caused contaminations with adjacent rocks, making unambiguous differentiation between MORB and island IAB additionally more problematic than it intrinsically is anyway (as Perfit and others, 1980, point out). None of the analyses (Table 2a) have abnormal Cr or Ni contents which excludes serpentinite contamination (compare Cr and Ni Table 2b samples 2-3).
The REE plots are typical for basalts (Pearce and Cann 1973; Kay and Hubbard 1978; Perfit et al. 1980; Hooper and Hawkesworth 1993) (Fig, 6a and 6b). They depict light REE (LREE), enhanced patterns, associated with IABs, and flat LREE-depleted patterns associated with MORB origins. An almost identical array of REE plots have been ascertained for the Northern Sporades where the present authors had drawn the conclusion that MORBs and IABs had been tectonically mixed

in the mélanges of an extensive thrust-fault zone (Fig. 7) (Scherreiks and BouDagher-Fadel 2020a). As in the Northern Sporades, the REE-plots drafted for the Vardar zone indicate the presence of both IAB and MORB (Fig. 7a-b). Discrimination diagrams (Fig. 7c) also indicate the ambiguous situation that MORBs for samples in one diagram correspond to IABs in another.

Following Perfit and others (1980) we have additionally checked out that according to Perfit (ibid) there are distinguishing differences in potassium, titanium, and total iron wt.% concentrations in IABs and MORBs: MORBs having <0.25 K_2O, IAB having >0.25 K_2O; IAB having <1.2 TiO_2, and >6-15 total Fe. The results of this query, using data from tables 2a and 2b, it appears that most of our samples are IABs but there are numerous ambiguities which, presumably, are caused by tectonic mélange mixing.

The analyses of the basalts from the Eohellenic ophiolite of Evvoia and those of the Elias complex are incorporated in the REE and AFM diagrams (Fig. 7a and c) (Table 2b) and they indicate MORB and IAB affinities.

Discussion and conclusions

The composite tectono-stratigraphy of eastern Pelagonia and the Vardar zone in context with the afore related geology

Pelagonia consists of a Palaeozoic-Middle Triassic basement covered by a carbonate platform over which a 200 km-wide ophiolite sheet of west Vardar ocean lithosphere, had been obducted (Fig. 8a, b, c). The 1700 km-wide eastern Vardar ocean subducted beneath the Vardar zone (vz) during Late Jurassic through Cretaceous time (Fig. 8c). Figure 8a - b suggests that Pelagonia together with obducted Eohellenic ophiolite collided with the Vardar zone and underthrusts the Cretaceous-carbonate-platform and its volcano-sedimentary substrate (Fig. 8 b). As Pelagonia continued to advance it underthrust the Guevgueli complex and crashed with Serbo-Macedonia (Fig. 8b, c).

Major deformations

Three major episodes of tectonic deformation, D1-D3, affected the Pelagonian and Vardar zones; each dominated by a major time-transgressive thrust fault complex (Fig. 8a-b). D1 and D2 occur in both study areas; D3 is evident in the Vardar zone but has not been verified in the Northern Sporades (Fig. 8a-b). (Our D1-D3 indices do not correspond with those of previous researchers (Mercier and Vergely 2002; Kilias et al. 2010; Katrivanos et al. 2013).

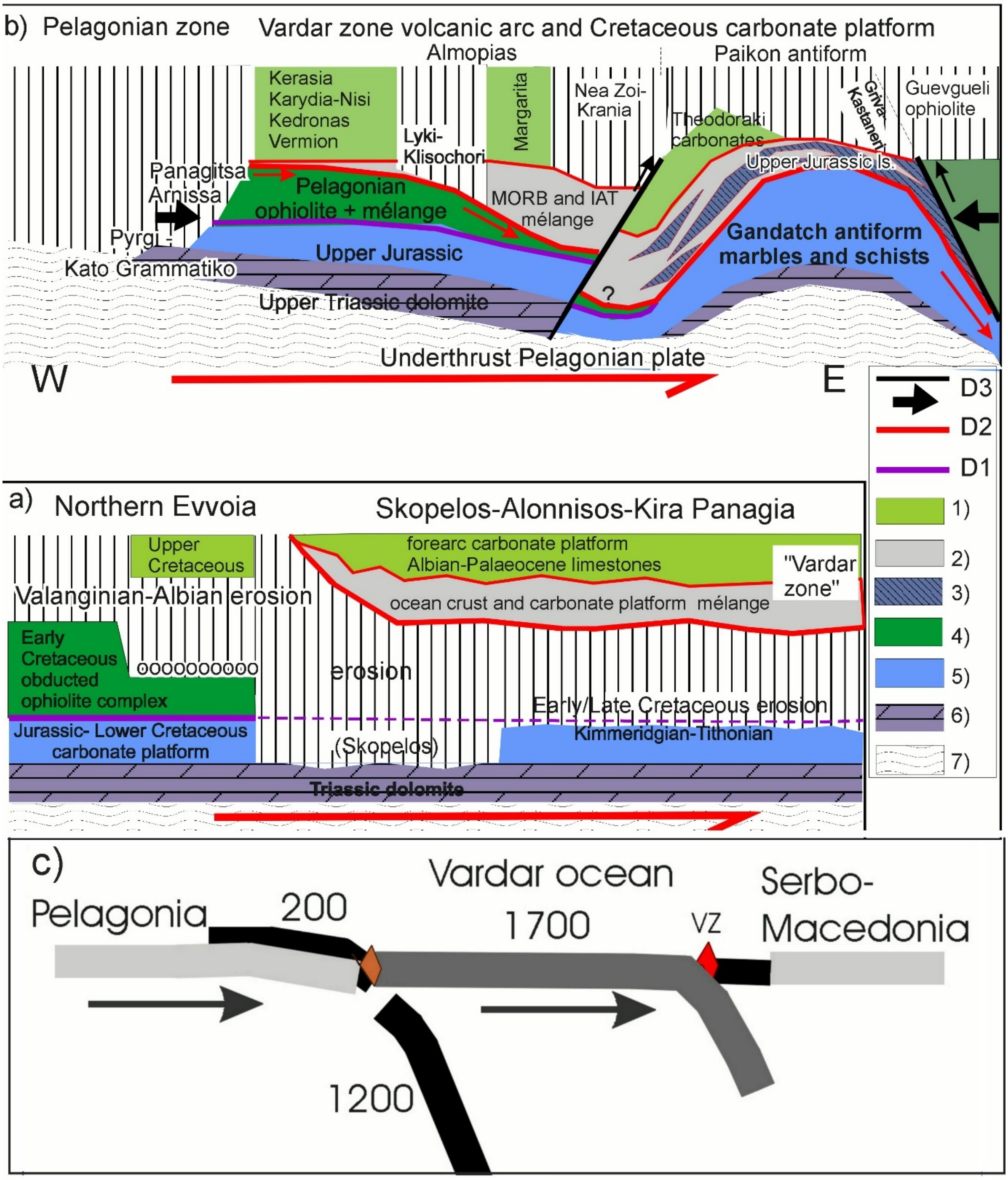

Fig. 8 (see figure captions)

Deformation D1, is Eohellenic (Fig. 8a), involving the westward obduction of the Eohellenic (west Vardar ocean) ophiolite onto eastern Pelagonia (Fig. 8c). Post-D1 erosion, especially prominent in Skopelos, is suggested to have been caused by widespread Pelagonian uplift as the sinking Vardar (1200km) slab broke off in post-Valanginian time (Fig.8c).

Deformation D2: Pelagonia, the trailing edge of the eastward subducting Vardar plate, crashed with and underthrust the Vardar arc, causing shearing, mylonitisation, and imbrication between the overriding Cretaceous carbonate platform including its volcano-sedimentary substrate. Greenschist and HP/LT metamorphism described by Katrivanous et al. 2013 can be attributed to D2.

Deformation D3 corresponds to the compression effected by the crash of the Pelagonian plate with Serbo-Macedonia, which caused folding in the Vardar and Pelagonian zones whereby the Paikon antiform is the most prominent (Fig. 8b). An analogical antiform has not been observed in the Northern Sporades but could be sought in the central Aegean sea (Fig. 8a). Shear-stress caused by the crash produced the youngest thrust faults in the flanks of the Paikon antiform (D3 in Fig. 8b) and most probably rejuvenated older faults, including numerous subordinate imbrication thrusts (Fig. 4b), described in Mercier and Vergely (2002), Kilias et al. (2010) and Katrivanos et al. (2013).

Pseudo conglomeratic mélange of Kedronas, Nisi and Karydia

The breccio-conglomeratic, cataclastic rock complex that contains abundant rounded clasts occurs incorporated in an extensive fault zone mélange in the west Almopias unit between Karydia and Ano Grammatiko (Plate 2a-b) (Fig. 6 pseudo conglomeratic mélange). In the Nisi-Karydia area the cataclasites are in tectonic contact with Campanian limestones on top (Plate 1) (Table 1b 4.1) and Pelagonian ophiolite at the base. We regard the cataclasites as matrix supported parabreccias composed of poorly sorted >2mm, rounded to angular clasts (Plate 2a-b). The clasts either consist predominantly of marbles, elongated pieces of sericitic calc-schists and dark micritic limestones (Plate 2b) or are chaotic mixtures of carbonate and ophiolite clasts (Plate 2a). Viewed under the microscope, the matrix is a chaotic breccia of calcite and carbonate grains that are not bound by interstitial pore cement (Bathurst 1976) but by insular patches of aggrading neomorphic sparry calcites that had grown amid the much smaller angular granules of the matrix (Plate 2c, d, e). Crushed neomorphic calcite occurs in the matrix inherited from earlier stages of shearing. The neomorphic calcite, unlike cement, exhibits irregular boundaries and palimpsest, relic-matrix texture (Plate 2 d-e). The neomorphic calcites exhibit residual stress, indicated by crossing twins, stopping twins, twin thickening, and bending, which appears in low temperature stress regimes below 200 °C. (Burkhard 1993; Chen et al, 2011). Neomorphism had most likely taken place in a dry sub-metamorphic environment (Folk 1965 in Bathurst 1976).

It is suggested that the larger components underwent rounding and grain-reduction by granulation from the decimetre to centimetre scale to microscopic micron scale, which is not unusual in tectonic breccias in which the fragments may be worn down and rounded by tectonic grinding (Norton 1917; Higgins 1971; Woodcock and Mort 2008).

We dispute that this rock complex had a transgressional origin (Mercier and Vergely 1988; and Mercier 1966 in Sharp and Robertson 2006) because it does not display the most important characteristics that marine conglomerates should have: clast-clast support and diagenetic cement (Bathurst 1976; Friedman 2006). On the contrary the clasts are matrix supported and the grains have not been diagenetically cemented.

In our opinion the “parabreccio-conglomerate” formed as Pelagonia underthrust the Vardar zone during Paleocene time (D2 above).

The collision of two Cretaceous carbonate platforms

It should be taken into consideration that some remnants of the well documented Cretaceous Pelagonian carbonate platform (Fig. 8a), may have been subducted (“piggy-backed”) beneath the Cretaceous carbonate platform of west Almopias, at the latest during Paleocene time, and thus inherited Pelagonian-orthoconglomerates possibly could occur in the mélanges beneath the Vardar zone (e.g., Vermion: Photiades et al. 2018).

New Paleogeography

From evidence presented above and from seismic tomography it is postulated that the Vardar ocean subducted along two subduction zones (Fig. 9a). The western intra-oceanic subduction zone evolved about Toarcian to Aalenian time, based on radiometric ages of amphibolites in sub-ophiolite mélanges, and continued to subduct through the Middle Jurassic verified by late Middle Jurassic radiolarians in the sub-ophiolite mélange in Evvoia (Danelian and Robertson 2001; Gingins and Schauner 2005; Scherreiks et al. 2014) (Table 1a 11.2 and 12). A supra-subduction volcanic arc evolved during the Middle Jurassic, documented by the Elias complex of northern Evvoia (Fig. 4a) which presumably was part of a more extensive supra-subduction “Eohellenic arc” (Fig. 9a) (ibid.). The beginning of the Eohellenic obduction, is suggested to have begun during Bathonian time together with the Callovian upheaval (Meléndez et al. 2007) and the eastward subduction of the eastern Vardar ocean (Fig. 9b3). The Vardar, supra-subduction, volcanic island arc and the spreading Guevgueli back arc ophiolite complex evolved during (Middle?) Late Jurassic and Cretaceous time. We envisage a Paikon forearc basin, rimmed by an accretionary wedge like that shown in Saccani et al. (2008b) in which the basin floor was initially covered by

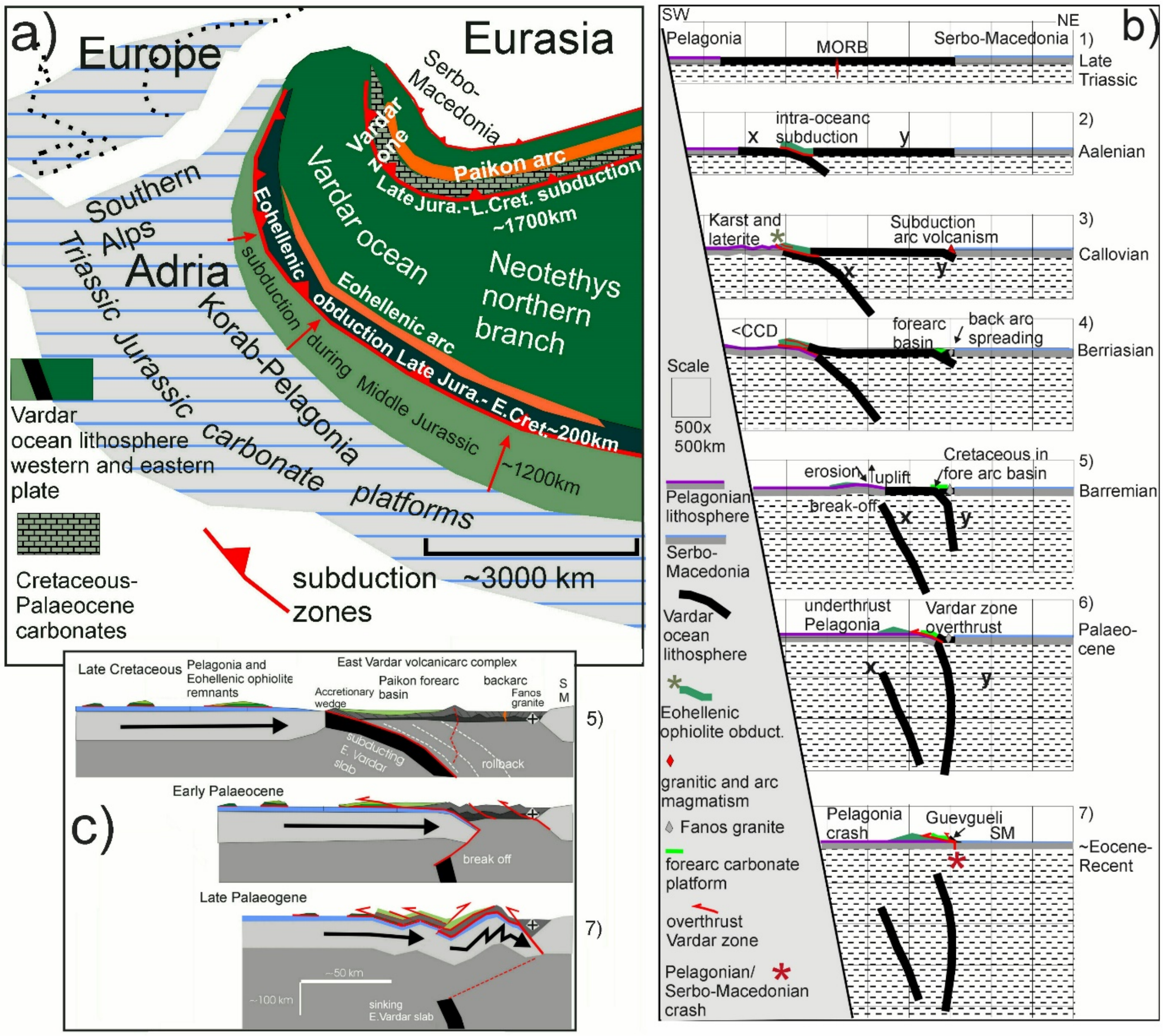

Fig. 9 (see figure cations)

(volcanoclastic) basalt without carbonates during the lower Middle Jurassic. To our knowledge, a Jurassic carbonate platform did not evolve in the Vardar zone. We suggest that Jurassic-early Cretaceous volcanoclastic deposits accumulated on the flanks of the Vardar volcanic arc and became the substrate of carbonate accumulation beginning in

Aptian time. Investigations of the Guevgueli back arc basin have not disclosed relicts of a carbonate platform (Saccani et al. 2008b).

The Cretaceous forearc carbonate platform of the Vardar zone

The Cretaceous Vardar-zone carbonate platform is envisaged to have evolved over the late Jurassic-early Cretaceous volcanoclastic substrate of the forearc basin (Fig. 9a) (Fig. 12 in Saccanni et al. 2008b).
The earliest recorded Cretaceous limestones in the Vardar zone are of Aptian age (Table 1b4.2, Table 1c6.1). The bio facies indicate a reefal to inner neritic environment having had depths of between 10 and 50m (BouDagher-Fadel 2018a). These limestones are in the west Almopias sub-zone (Fig. 4b) and may have been deposited near or on the accretionary wedge of the forearc basin (Saccani et al. 2008b). The verified bio facies indicate that patch reef and neritic environments existed side by side through Cenomanian, Santonian, Campanian, and Maastrichtian time (Table 1b West Almopias) (Plate 1). The deeper neritic platform facies occur eastwards in the central and east Almopias sub zones, ranging in age from the Cenomanian to Maastrichtian (Table 1b-c Central and East Almopias). The bio stratigraphic succession in the Theodoraki limestone formation begins with Cenomanian/Turonian reef facies that may represent a fringing reef along the outer slopes of the arc. Inner neritic facies deepen upwards, from the Campanian to Maastrichtian times (Table 1c 5 Theodoraki unit). Late Maastrichtian flysch signals the demise of the Cretaceous carbonate platform of the Vardar zone.
From the afore said, a tentative picture of the platform-architecture can be discerned: it was a subsiding environment in which about 500 m of carbonates accumulated ("carbonate factory" Schlager 2000) during about 60Ma between Aptian and Maastrichtian time (Mercier and Vergely 1984, 1988). Reefs evolved during Early Cretaceous along an outer western accretionary wedge and inner eastern high where fringing reefs on the outer slopes of the Paikon volcanic arc interdigitated outer neritic carbonate facies in the central basin.

Seismic tomographic images of the mantle below the Hellenides

We have interpreted the perturbations beneath Hellenides as sunken Vardar ocean lithosphere which indicate two episodes of subduction (Scherreiks and BouDagher-Fadel 2020a) (Fig. 3c).
The vertical section (Fig. 3c) shows that the leading edges of each slab has sunk to a depth approaching 2000 kilometres. Presently, the trailing

edge of the western slab (x in Fig. 3c) is about 900 kilometres below the Earth´s surface and the trailing edge of slab (y) is about 400 kilometres below the surface. These are the depths to which the slabs have sunk since their breakoffs. In estimating the width of a slab, however, one must consider that a subsiding lithospheric plate certainly undergoes compression and deformation which can make width-estimates inaccurate (Fig 3e). The seismic tomographic images are, nevertheless, presently the best possible way to estimate the onetime width of the subducted oceanic lithosphere which we estimate to have been about 3000 kilometres (determined by adding together the lengths of the slabs (x + y) ~1200 + ~1700 and adding, to that sum, the width of the obducted Eohellenic ophiolite sheet which has been assumed to be about ~200 kilometres (Fig. 8c)). However, 3100km is the composite width, not necessarily the surface width that the Vardar ocean had at any one time. We do not know when the ocean ridge stopped spreading: subduction and ocean spreading at the ocean ridge could have taken place simultaneously.
The western slab (x) is supposed to have broken off and began sinking after the Eohellenic ophiolite had been emplaced during Valanginian time. The eastern Almopias slab (y) is supposed to have broken off after Pelagonia crashed and underthrust the Vardar-zone carbonate platform and volcanic arc complex.

Seismic tomographic model

Our model (Fig. 9) postulates that the Vardar ocean was about 3000km wide and bordered on Adria in the west. This means that both the microplate Adria and the vaguely attached African plate, were situated 3000km further southwest during Early Jurassic time as the Atlantic Ocean and the Alpine Tethys began spreading (e.g., Schmid et al. 2008; Scherreiks et al. 2010). This implies that Pelagonia, the eastern edge of Adria, moved about 3000km northeast towards the European continent (Fig. 9b) while the Atlantic spread.
The ~3000km wide Vardar ocean is supposed to have subducted/obducted, between (~Sinemurian) Aalenian time (175 Ma) and Paleocene time (~65 Ma), roughly a time span of 175 - 65 = 110Ma. Subduction rates of the oceanic slabs are estimated to range from about 3 cm/year (= 30km/1Ma) in the upper mantle to about 1 cm/year in the lower mantle (Norton 1999). Simple calculations show that at a rate of 30km/1Ma, a 3300km wide ocean would subduct in 110 Ma; and a 3000km wide ocean could subduct in 110Ma at a rate of ~2.7cm/a.

In our example, we also consider that the trailing edge of Slab X sank 900 km since breaking off after Valanginian time, and the trailing edge of slab Y sank about 400 km since its breakoff in the ~Paleocene. Sinking rates are lower in the mantle below 300–500 km, and in the lower mantle slab subsidence eventually approaches zero (Lallemand and Funiciello 2009; Ichikawa et al. 2016). We have previously estimated (Scherreiks and BouDagher-Fadel 2020a. 2020b) that in using an average subsidence rate of 0.68 cm/year, one arrives at a Hauterivian break-off date for slab X (900km/6.8km/Ma ~132 Ma), and Late Paleocene as the break-off time of slab Y (400 km/6.8 km/Ma ~59 Ma), which we believe corresponds to the known facts and is well in the range of plausibility.

Summary

The demise of the once over 3000-kilometre-wide Vardar ocean has been reconstructed from field investigations of its remnants in its onetime peripheries, and from seismic tomographic images of its remnants in the Mantle below the Central Hellenides. On its southwestern side the Vardar ocean bordered on the Pelagonian-Adriatic plate which was covered by a vast carbonate platform (BouDagher-Fadel and Bosence 2007) that evolved from a peritidal realm during Norian-Sinemurian- to a drowned platform during Tithonian-Berriasian-time. In the northeast the Vardar ocean bordered on Serbo-Macedonia of the European plate, where, during the Late Jurassic a supra-subduction volcanic island arc and back-arc complex emerged. A forearc reef and a shallow marine carbonate platform accumulated on top of a Jurassic-early Cretaceous volcano-clastic substrate from about Aptian through Maastrichtian time.
The closure of the Vardar ocean occurred in temporally overlapping episodes: one episode of ophiolite obduction and two episodes of intra-oceanic subduction.

1. During Middle Jurassic time a 1200-kilometre slab of west Vardar lithosphere subducted eastwards beneath the “Eohellenic”, arc, while a 200-kilometre-wide slab obducted westwards onto Pelagonia between Callovian and Valanginian time.
2. A 1700-kilometre-wide slab of east Vardar lithosphere subducted eastwards beneath the Vardar-zone arc-complex during Late Jurassic through Cretaceous time and subsequently Pelagonia underthrust the Cretaceous carbonate platform during the Paleocene.

In the greater framework of plate tectonics, the subduction of the Vardar ocean occurred simultaneously with the spreading of the Atlantic Ocean and the opening of the Alpine Tethys, while the Hellenides moved about 3000 kilometres toward the northeast.

In the light of the present contribution, future research concerning the evolution of the Cretaceous carbonate platform of the Vardar zone could advance our knowledge of the facies distributions and architecture of the Paikon fore arc basin. Another point of interest is the seismic tomography and the demise of the Guevgueli back arc since Paleocene time.

Acknowledgements

University College London:

We are grateful to the Office of the Vice-Provost (Research, Innovation, and Global Engagement), especially Prof. David Price, for helping and facilitating our research.

The *Bayerische Staatssammlung für Palaeontologie und Geologie and the Department of Earth and Environmental Sciences,* Ludwig Maximilian University, Munich, through Prof. Anke Friedrich and Dr. Winfried Werner, are acknowledged for supporting this research which turned out to become an over 20-year project for which we gratefully thank Prof. Peter Baumgartner (Lausanne), Prof. Dan Bosence (London), Dr. Georgia Fermeli (Athens) and Prof. Guillermo Meléndez (Saragossa) for their most valued previous field and co-author participations. We thank ACTIVATION LABORATORIES LTD., Ancaster, Ontario, for carrying out the geochemical analyses. Special thanks are given Michael Born, Bonn, Germany for the preparation of thin sections. We are indebted to Prof Robert Hall, Royal Holloway, University of London, for carefully and thoroughly reviewing our paper.

References

Anders, B., Reischmann, T., Poller, U., Kostopoulos, D. (2005) Age and origin of granitic rocks of the eastern Vardar Zone, Greece: new constraints on the evolution of the Internal Hellenides. J. Geol. Soc. London, 162: 857-870.

Bathurst, R. G. C. (1976) Carbonate sediments and their Diagenesis. Dev in Sedimentol 12, Elsevier, 658pp

Baumgartner P. O., Bernoulli D. (1976) Stratigraphy and radiolarian fauna in a Late Jurassic–Early Cretaceous section near Achladi (Evvoia, Eastern Greece). Ecl Geol Helv 69:601–626

Baumgartner, P.O., Bartolini, A., Carter, E.S., Conti, M., Cortese, G., Danelian, T., De Wever, P., Dumitrica, P., Dumitrica-Jud, R., Gorican, S., Guex, J., Hull, D.M., Kito, N., Marcucci, M., Matsuoka, A., Murchey, B., O'Dogherty, L., Savary, J., Vishnevskaya, V., Widz, D. and Yao, A., (1995) Middle Jurassic to early cretaceous radiolarian biochronology of Tethys based on unitary associations. In: Baumgartner, P.O. et al., eds., Middle Jurassic to lower cretaceous Radiolaria of Tethys: occurrences, systematics, biochronology, Mém. Géol., (Lausanne), 23, 1013-1048.

BeBien, J., Voet, P. B., Mercier, J. (1994): Geodynamic significance of the Paicon massif in the Hellenides: Contribution of the volcanic rock studies. Bulletins of the Geological Society of Greece, 30/1: 63-67.

Bernoulli, D., Manatschal, G., Desmurs, L., Müntener, O. (2003) Where did Gustav Steinmann see the trinity? Back to the roots of an Alpine ophiolite concept. in Dilek, Y., and Newcomb, S., eds., Ophiolite concept and the evolution of geological thought: Boulder, Colorado, Geological Society of America Special Paper 373, p. 93–110.

Bijwaard, H., Spakman, W. (2000) Non-linear global P-wave tomography by iterated linearized inversion. Geophys. J. Int. 141, 71-82

Bijwaard, H.W., Spakman, W., Engdahl, E.R. (1998) Closing the gap between regional and global travel time tomography. J. Geophys. Res, 103, 30,055–30,078

Bortolotti, V., Chiari, M., Marroni, M., Pandolfi, L., Principi, G., Saccani, E. (2013) Geodynamic evolution of ophiolites from Albania and Greece (Dinaric-Hellenic belt): one, two, or more oceanic basins? Int J Earth Sci 102:783-811

Bosellini, A. (1984) Progradation geometries of carbonate platforms: examples from the Triassic of the Dolomites, northern Italy. Sedimentology, 31, 1-24

Bosence, D. (2005) A genetic classification of carbonate platforms based on their basinal and tectonic settings in the Cenozoic. Sediment Geol 175:49–72

Bosence, D., Procter, E., Aurell, M., Atef Bel, K., BouDagher-Fadel, M., Casaglia, F., Cirilli, S., Mehdie, M., Nieto, L., Rey, J., Scherreiks, R., Soussi, M. and Waltham, D., (2009) A dominant tectonic signal in high-frequency, peritidal carbonate cycles? A regional analysis of Liassic platforms from western Tethys, J. Sed. Res., 79(5-6), 389-415.

BouDagher-Fadel, M.K., Bosence, D.W.J. Early Jurassic benthic foraminiferal diversification and biozones in shallow-marine carbonates of western Tethys. Senckenbergiana lethaea 87, 1–39 (2007).

BouDagher-Fadel, M. K. (2008) The Mesozoic larger benthic foraminifera: the Jurassic. In: Boudagher-Fadel, M.K., ed., Evolution and geological significance of larger benthic foraminifera, Wignall PB (series ed) Dev Palaeontol Strat 21, Elsevier, Amsterdam.

BouDagher-Fadel, M.K., (2015) Biostratigraphic and Geological Significance of Planktonic Foraminifera (Updated 2nd Edition). London: UCL Press. doi:10.14324/111.9781910634257.

BouDagher-Fadel, M.K. (2018a) Evolution and Geological Significance of Larger Benthic Foraminifera, Second ed. UCLPress, London. 704 pp.

BouDagher-Fadel, M. K. (2018b) Revised diagnostic first and last occurrences of Mesozoic and Cenozoic planktonic foraminifera. UCL Office of the Vice-Provost Research, Professional Papers Series, 1-5.

BouDagher-Fadel, M., & Price, G. D. (2019) Global evolution and paleogeographic distribution of mid-Cretaceous orbitolinids. UCL OPEN - ENVIRONMENT. doi:10.14324/111.444/ucloe.000001

Brown, S., Robertson, A. (1994) New structural evidence from the Mesozoic-early Tertiary Paicon unit, Northern Greece. Bull Geol Soc Greece, 30/1: 159-170

Brown, S.A.M., Robertson, A.H.F. (2004) Evidence for Neotethys rooted within the Vardar suture zone from the Voras Massif, northernmost Greece. Tectonophysics 381, 143e173.

Burkhard, M. (1993) Deformation mechanisms and fabric Calcite twins, their geometry, appearance and significance as stress-strain markers and indicators of tectonic regime: a review. Jour of Structural Geol, 15, 3–5, 351-368

Chen, K., Kunz, M., Tamura, N. et al. (2011) Deformation twinning and residual stress in calcite studied with synchrotron polychromatic X-ray microdiffraction. Phys Chem Minerals 38, 491–500

Chiari, M., Marcucci, M. (2003) Triassic and Jurassic radiolarian assemblages from the siliceous sediments associated with pillow lavas in the Argolis Peninsula (Greece). Abstr Tenth Meeting International Association Radiolarian Palaeontologists, Lausanne: 40

Chiari, M., Bortolotti, V., Marcucci, M., Photiades, A., Principi, G., Saccani, E. (2012) Radiolarian biostratigraphy and geochemistry of the Koziakas massif ophiolites (Greece). Bull. Soc. géol. France,183, no 4, 289-309.

Danelian, T., Robertson, A.H.F. (2001) Neotethyan evolution of eastern Greece Pagondas Mélange, Evia island inferred from radiolarian biostratigraphy and the geochemistry of associated extrusive rocks. Geol Mag 138:345–363

Fazzuoli, M., Menna, F., Nirta, G., Bortolotti, V., Carras, N., Principi, G. (2008) The Cretaceous transgression in the Dinaric-Hellenic orogen. Soc. Geol. It., 6, Nuova Serie

Flügel, E. (1974) Fazies-Interpretation der Cladocoropsis-Kalke (Malm) auf Karaburun, W-Anatolien. Arch Lagerstforsch (Ostalpen) Sonderbd 2, Leoben, 79-94

Flügel, E. (1983) Mikrofazies der Pantokrator-Kalke (Lias) von Korfu, Griechenland. Facies 8: 263-300

Friedman, G.M. (2003) Classification of sediments and sedimentary rocks. In Gerard V. Middleton, ed., pp. 127-135, Encyclopedia of Sediments & Sedimentary Rocks, Encyclopedia of Earth Science Series. Kluwer Academic Publishers, Boston, Massachusetts. 821 pp. ISBN 978-1-4020-0872-6

Froitzheim, N., Jahn-Awe, S., Frei, D., Wainwright, A.N., Maas, R., Georgiev, N., Nagel, J.T., Pleuger, J. (2014) Age and composition of meta-ophiolite from the Rhodope Middle Allochthon (Satovcha, Bulgaria): a test for the maximum-allochthony hypothesis of the Hellenides. Tectonics 33(8):1477–1500

Fruth, I., Scherreiks, R. (1982) Hauptdolomit (Norian) – sratigraphy, paleogeography and diagenesis. Sedimentary Geol, 32: 195-231

Gallhofer, D., von Quadt, A., Schmid, S.M., Guillong, M., Peytcheva, I., Seghedi, I. (2017) Magmatic and tectonic history of Jurassic ophiolites and associated granitoids from the South Apuseni Mountains (Romania). Swiss J. Geosci. 110, 699-719

Gawlick, H-J., Frisch, W., Hoxha, L., Dumitrica, P., Krystyn, L., Lein, R., Missoni, S., Schlagintweit, F. (2008) Mirdita zone ophiolites and associated sediments in Albania reveal Neotethys ocean origin. Int J Eartg Sci (Geol Rundsch) 97:865–881

Georgiadis, G.A., Tranos, M.D., Kilias, A.A., Mountrakis, D.M. (2016) The emplacement of the Vermion nappe in the area of Kato Seli (Mt. Vermion Central Macedonia, Greece. Bull. Geol. Soc. Greece, vol. L, 24-33 Proceed.14th Intern. Congr. Thessaloniki

Gingins, Y., Schauner, O. (2005) Etude ge´ochimique et paleontologique des series Maliaques d'Othrys et du complexe d'Elias, Eubee du Nord, Grece. Diss Universite´ de Lausanne, Manuscript February 2005, 1–93pp

Hafkenscheid, E. (2004) Subduction of the Tethys Oceans reconstructed from plate kinematics and mantle tomography. Thesis, Faculty of Geosciences Utrecht University, The Netherlands. ISBN: 90-5744- 101-200.

Higgins, M.W. (1971) Cataclastic Rocks. Geol Surv Professional Paper 687, U S Government Print Office, Washington Library of Congress Catalog No. 71-611932; 1971.

Hooper, P.R., Hawkesworth, C.J. (1993) Chemical characteristics of island arc basalts. J Petrol. 1993; 34:1203–46

Hsü, K.J. (1974) Melanges and their distinction from olistostromes. In: Dott RH, Shaver RH (eds) Modern and ancient geosynclinal sedimentation. Soc Econ Paleontol Mineral Spec Publ 19: 321-333

Ichikawa, H., Yamamoto, S., Kawai, K., Kameyama, M. (2016) Estimate of subduction rate of island arcs to the deep mantle. J Geophys Res Solid Earth. 2016; 121:5447–60.

Jacobshagen, V., Risch, H., Roeder, D. (1976) Die Eohellenische Phase. Definition und Interpretation. Zeitschr Deutsche Geol Gesell. 1976;127: 133–45.

Jacobshagen, V., (1986) Geologie von Griechenland. In: Beiträge Zur Regionalen Geologie der Erde Band 19. Gebrüder Bornträger, Berlin, 363 pp

Katrivanos, E., Kilias, A., Mountrakis, D. (2013) Kinematics of deformation and structural evolution of the Paikon Massif (Central Macedonia, Greece): A Pelagonian tectonic window? N. Jb. Geol. Paläont. Abh. 269/2, 149–171

Kay, R.W., Hubbard, N.J. (1978) Trace elements in ocean ridge basalts. Earth Planet Sci Lett. 38:95–116.

Kelepertsis, A. (1974) Geological structure of Alonnisos and Peristera islands. Z dt geol Ges;125: 225–36.

Kendall, G.St.C., Schlager, W. (1981) Carbonates and relative changes in sea level. In: Cita MB, Ryan WBF (eds) Carbonate platforms of the passive-type continental margins, present and past. Mar Geol 44: 181–212

Kilias, A., Frisch, W., Avgerinas, A., Dunkl, I., Falalakis, G., Gawlick, H-J. (2010) Alpine architecture and kinematics of deformation of the northern Pelagonian nappe pile in the Hellenides. Austrian Journal of Earth Sciences Volume 103/1 4-28

Kockel, F. (1979) in: Die Vardar- (Axios-) Zone. Jacobshagen, V., Geologie von Griechenland, Gebrüder Borntraeger Berlin-Stuttgart, pp. 150-168.

Lallemand, S., Funiciello, F., (2009) editors: Royden, Leigh H. (et al.) Subduction with Variations in Slab Buoyancy: Models and Application to the Banda and

Apennine Systems. Subduction zone geodynamics; 35. Springer-Verlag, Berlin, Heidelberg, 272pp. ISBN 978-3-540-87974-9
Matarangas, D. (1992) Geological investigations of Skopelos island (North Sporades, Greece). D 188 (Diss. Freie Universität Berlin) Berichte des Forschungszentrums Jülich, 2684,157.
Meléndez, G., Ramajo, J., Bello, J., D'Arpa, C., Di Stefano, P., Fermeli, G., Karakitsios, V., Mallarino, G., Mindszenty, A., Scherreiks, R., Zarcone, G. (2007) Palaeogeographic and palaeontologic event across the Tethys, in the Submediterranean and Mediterranean platforms at the Callovian-Oxfordian transition. XXIII Jornadas de la Sociedad Espanola de Paleontologia (Caravaca de la Cruz, Libro de Resumenes:139–140
Meneghini, F., Marroni, M., Moorw, J.C., Pandolfi, L., Rowe, C.D. (2009) The processes of underthrusting and underplating in the geologic record: structural diversity between the Franciscan Complex (California), the Kodiak Complex (Alaska) and the Internal Ligurian Units (Italy). Geol. J. 44: 126–152
Mercier, J. (1968) Etude geologique des zones Internes des Hellenides en Macedoine centrale. Contribution à l'étude du metamorphisme et de l' évolution magmatique des zones internes des Hellenides. – Annales Géologique des Pays Hélléniques 20, 1-739.
Mercier, J., Vergely, P., Geological Map of Greece 1.50.000 - Sheet Arnissa (1988) Institute of Geology and Mineral Exploration, Athens
Mercier, J., Vergely, P., Geological Map of Greece 1.50.000 - Sheet Edhessa (1984) Institute of Geology and Mineral Exploration, Athens
Mercier, J. L., Vergely, P. (1972) Le mélanges ophiolitiques de Macédoine (Grèce) : décrochements d'âge anté-Crétacé supérieur. Z. Deutsch, geol. Ges., Hannover, 123, 469-489.
Mercier, J.L., Vergely, P., 2002. The Paikon massif revisited, comments on the Late Cretaceous e paleogene geodynamics of the Axios-Vardar Zone. How many Jurassic ophiolitic basins? (Hellenides, Macedonia, Greece). Bull. Geol. Soc. Greece 34/6, 2099-2112. doi: org/10.12681/bgsg.16852.
Michail, M., Pipera, K., Koroneos, A., Kilias, A., Ntaflos, T. (2016) New perspectives on the origin and emplacement of the Late Jurassic Fanos granite, associated with an intra-oceanic subduction within the Neotethyan Axios-Vardar Ocean. Published online: 26 March 2016 Springer-Verlag Berlin Heidelberg 2016
Norton, W.H. (1917) A Classification of Breccias. The Journal of Geology, Vol. 25, No. 2, 160-194
Norton, I. O. (1999) Global plate reconstruction model report. Texas (USA): Exxon Mobil Exploration
Pearce, J.A., Cann, J.R. (1973) Tectonic setting of basic volcanic rocks determined using trace element analyses. Earth Planet Sci Lett. 1973; 19:290–300.
Perfit, M.R., Gust, D.A., Bence, A.E., Arculus, R.J., Taylor, S.R., (1980) Chemical characteristics of island-arc basalts: Implications for mantle sources. Chemical Geology Volume 30, Issue 3, 227-256
Photiades, A., Carras, N., Bortolotti, V., Fazzuoli, M. (2018) The late Early Cretaceous transgression on the laterites in Vourinos and Vermion massifs (western Macedonia, Greece). Bulletin of the Geological Society of Greece 40(1):182

Robertson, A. (2004) Development of concepts concerning the genesis and emplacement of Tethyan ophiolites in the Eastern Mediterranean and Oman regions. Earth Sci Rev 66:331–387

Robertson, A.H.F., Trivić, B., Đerić, N., Bucur, I. (2013) Tectonic development of the Vardar ocean and its margins: Evidence from the Republic of Macedonia and Greek Macedonia. Tectonophysics 595–596, 25–54

Roddick, J.C., Cameron, W.A., Smith, A.G. (1979) Permo-Triassic and Jurassic 40Ar/39Ar ages from Greek ophiolites and associated rocks. Nature 279:788–790

Saccanni, E., Photiades, A., Santato, A., Zeda, O. (2008a) New evidence for supra-subduction zone ophiolites in the Vardar zone of northern Greece: Implications for the tectonic-magmatic evolution of the Vardar ocean basin Ofioliti, 2008, 33 (1), 65-85

Saccanni, E., Bortolotti, V., Marroni, M., Pandolfi, L., Photiades, A., Principi, G. (2008b) The Jurassic association of backarc basin ophiolites and calc-alkaline volcanics in the Guevgueli complex (Northern Greece): Implications for the evolution of the Vardar Zone. Ofioliti 33 (2), 209-227

Saccani, E., Chiari, M., Bortolotti, V., Photiades, A., Principi, G. (2015) Geochemistry of volcanic and subvolcanic rocks and biostratigraphy on radiolarian cherts from the Almopias ophiolites and Paikon unit (Western Vardar, Greece). Ofioliti 40,1-25. https://doi.org/10.4454/ofioliti.v40i1.432.

Scherreiks, R. (1998) The evolution of a passive margin in response to plate tectonics, eustacy, and an advancing ophiolite nappe (Jurassic, NE-Evvoia, Greece). Terra Nostra 98: 72-73

Scherreiks, R. (2000) Platform margin and oceanic sedimentation in a divergent and convergent plate setting (Jurassic, Pelagonian Zone, NE Evvoia, Greece). Int J Earth Sci 89:90–107

Scherreiks, R., Bosence, D., BouDagher-Fadel, M., Meléndez, G., Baumgartner, P.O. (2010) Evolution of the Pelagonian carbonate platform complex and the adjacent oceanic realm in response to plate tectonic forcing (Late Triassic and Jurassic), Evvoia, Greece. Int J Earth Sci 99:1317–1334

Scherreiks, R., Meléndez, G., Fermeli, G., Baumgartner, P.O., BouDagher-Fadel, M., Bosence, D. (2011) A time-transgressive ophiolite-platform collision (late Middle Jurassic to Early Cretaceous, Pelagonian zone, Evvoia, Greece). Fragile Earth: GV-GSA meeting, LMU München Paper 19-9

Scherreiks, R., Meléndez, G., BouDagher-Fadel, M., Fermeli, G., Bosence, D. (2014) Stratigraphy and tectonics of a time-transgressive ophiolite obduction onto the eastern margin of the Pelagonian platform from Late Bathonian until Valanginian time, exemplified in northern Evvoia, Greece, Int. J. Earth Sci., 103, 2191-2216.

Scherreiks, R., Meléndez, G., BouDagher-Fadel, M., Fermeli, G., Bosence, D. (2016) The Callovian unconformity and the ophiolite obduction onto the Pelagonian carbonate platform of the Internal Hellenides. Bulletin of the Geological Society of Greece, vol. L; Proceedings of the 14th Intern. Congress, Thessaloniki, May 2016

Scherreiks, R., BouDagher-Fadel, M. (2020a) Tectono-stratigraphic correlations between Northern Evvoia, Skopelos and Alonnisos, and the postulated collision of the Pelagonian carbonate platform with the Paikon forearc basin (Pelagonian-Vardar zones, Internal Hellenides, Greece). UCL Open

Scherreiks, R., BouDagher-Fadel, M. (2020b) The closure of the Neotethys in two episodes: as a result of Late Jurassic to Early Cretaceous obduction and Early Paleocene collision, based on surface geology and tomographic models (Internal Hellenides, Greece) Conference: Tectonics, geodynamics, and paleogeography of the Alpine-Himalayan orogen from the Earth´s mantle to its surface at: Utrecht virtual oral presentation 26.08.2020 Session 3.3 ID 112

Schmid, S.M., Bernoulli, D., Fügenschuh, B., Matenco, L., Schefer, S., Schuster, R., et al. (2008) The Alpine-Carpathian-Dinaridic orogenic system: correlation and evolution of tectonic units. Swiss J Geosci. 101:139–83.

Schmid, S.M., Fügenschuh, B., Kounov, A., Matenco, L., Nievergelt, P., Oberhänsli, R., et al. (2020) Tectonic units of the Alpine collision zone between Eastern Alps and western Turkey. Gondwana Res. 78:308–374.

Sengör, A.M.C., Natal´in, B.A. (1996) Paleotectonics of Asia: fragments of a synthesis, in: The Tectonic Evolution of Asia, eds Yin A, Harrison T.M., 486–640, Cambridge University Press.

Sharp, I.R., Robertson, A.H.F. (1994) Late Jurassic–Lower Cretaceous oceanic crust and sediments of the eastern Almopias Zone, NW Macedonia (Greece); implications for the evolution of the eastern ‘‘Internal’’ Hellenides. Bull Geol Soc Greece 30:47–61

Sharp, I. R. & Robertson, A. H. F. (1998) Late Jurassic-Lower Cretaceous oceanic crust and sediments of the Eastern Almopias Zone, NW Macedonia (Greece); implications for the evolution of the Eastern 'Internal' Hellenides. Bulletin of the Geological Society of Greece, 30(1), 47-61.

Sharp, I.R., Robertson, A.H.F. (2006) Tectonic-sedimentary evolution of the western margin of the Mesozoic Vardar Ocean: evidence from the Pelagonian and Almopias zones, northern Greece. In: Tectonic development of the Eastern Mediterranean Region. Robertson AHF, Mountrakis D (Eds.), Geol. Soc. London Spec. Publ., 260: 373-412.

Simantov, J., Economou, C., Bertrand, J. (1991) Metamorphic rocks associated with the Central Euboea ophiolite (southern Greece): some new occurrences. In: Malpus J, Moores EM, Panayiotou A, Xenophontos C (eds) Ophiolites, oceanic crustal analogies. Proc Symp Troodos 1987, Geol Surv Dept Nicosia/Cyprus, pp 285-293

Schlager, W., (2000) Sedimentation rates and growth potential of tropical, cool-water and mud-mound carbonate systems. In Insalaco, E., Skelton, P. W., and Palmer, T. J. (eds.), Carbonate Platform Systems: Components and Interactions. London: The Geological Society, pp. 217–227.

Spakman, W., van der Lee, S., van der Hilst, R.D. (1993) Travel-time tomography of the European^Mediterranean mantle down to 1400 km, Phys. Earth planet. Inter., 79, 3-74.

Spray, J.G., Roddick, J.C (1980) Petrology and Ar geochemistry of some Hellenic subophiolite metamorphic rocks. Contrib Mineral Petrol72:43–55

Spray, J.G., Bebien, J., Rex, D.C., Roddick, J.C. (1984) Age constraints on the igneous and metamorphic evolution of the Hellenic±Dinaric ophiolites. Geol Soc Lond Spec Publ 17 : 619±627

Stais, A., Ferriere, J., Caridroit, M., De Wever, P., Clement, B., Bertrand, J. (1990) Donnees nouvelles sur l'histoire ante-obduction (Trias- Jurassique) du domaine d'Almopias (Macedoine, Grece). Comptes Rendus de l'Academie de Sciences, Serie II, 310, 1275-1480.
Stampfli, G.M., Borel, G.D. (2004) The TRANSMED transects in space and time: Constraints on the paleotectonic evolution of the Mediterranean domain, in The TRANSMED Atlas: the Mediterranean Region from Crust to Mantle. eds Cavazza, W., Roure, F., Spakman, W., Stampfli, G.M., Ziegler, P.A., Springer
Tranos, M. D., Plougarlis, A. P., Mountrakis, D. M. (2007) A new consideration about the Almopias-Paikon boundary based on the geological mapping in the area of Nerostoma-Lakka (Central Macedonia, Greece) Proceedings of the 11t h International Congress, Athens, May,
Ustaszewski, K., Kounov, A., Schmid, S.M., Schaltegger, U., Krenn, E., Frank, W., Fügenschuh, B. (2010) Evolution of the Adria-Europe plate boundary in the northern Dinarides: from continent–continent collision to back-arc extension. Tectonics 29:1-34
van der Meer, D.G., van Hinsbergen, D.J.J., Spakman, W. (2018) Atlas of the underworld: Slab remnants in the mantle, their sinking history, and a new outlook on lower mantle viscosity. Tectonophysics 723, 309–448
van Hinsbergen, D.J.J., Hafkenscheid, E., Spakman, W., Meulenkamp, J.E., Wortel, M.J.R. (2005) Nappe stacking resulting from subduction of oceanic and continental lithosphere below Greece. Geology 33, 325–328.
van Hinsbergen, D.J.J., Torsvik, T.H., Schmid, S.M., Matenco, L.C., Maffione, M., Gürer, D., Vissers, R.L.M. (2019) Companion paper. Orogenic architecture of the Mediterranean region and kinematic reconstruction of its tectonic evolution since the Triassic. Gondwana Res.
Vermeesch, P. (2006) Tectonic discrimination diagrams revisited. Geochem Geophys Geosyst Am Geophys Union 7(6):1–55
Woodcock, N.H., Mort, K. (2008). Classification of fault breccias and related fault rocks. Geological Magazine, 145(3), 435-440.
Zimmerman, J., Ross, J.V. (1976) Structural evolution of the Vardar root zone, northern Greece. Bull Geol Soc Am 87: 1547-1550

Figure Captions

Fig. 1: Neotethys lithosphere oceanic lithosphere in the Dinarides through the Hellenides and Taurides, represent remnants of the northern branch of the Neotethys (altered after Ustaszewski et al. 2010). Our study areas are in Evvoia and the Northern Sporades, and in the “Vardar zone” of Greek Macedonia. Fieldwork was carried out in the Vardar zone and Northern Evvoia in September and October 2020 and Evvoia and the Northern Sporades in previous years.

Fig. 2 Paleogeography and evolution of the Vardar ocean (a) altered after Stampfli and Borel, 2004; (b) altered after Schmid et. al. 2008; Gallhofer et al 2017 and Van Hinsbergen et al. 2019, in Schmid et al, 2020)
a) The Vardar domain of the Northern Tethys ocean evolved out of the Maliac and Paleotethys in Permo-Triassic time.
b) The Vardar ocean was situated between continental Adria (including Korab-Pelagonia) and Serbo-Macedonian Europe. The paleogeography implies that early Middle Jurassic intra-oceanic subduction led to the obduction of the Eohellenic ophiolite onto eastern Pelagonia and, subsequently, that Vardar

ocean lithosphere subducted beneath the Paikon island arc and led to the collision of eastern Pelagonia with the island arc. See text.

Fig. 3 Seismic tomographic images below the Central Hellenides

a) Map sketch of the Hellenides shows the position of the NE-SW vertical section through the mantle below the Central Hellenides c).

b) Seismic tomographic images (BSE models, ascertained from Hafkenscheid 2004) of horizontal sections through the mantle at 6 different depths. They depict contours of seismic velocity anomalies (see Hafkenscheid 2004 for the theoretical background).

c) The vertical section through the BSE models. The sketch schematically depicts perturbation "clouds" containing the lithospheric "slabs" (see e)). Slab X has sunk about 900km, slab Y has sunk about 400km.

d) Vertical sections depicting the mantle eastwards of the Hellenides show that there are two sinking lithospheric slabs. Positions of sections are shown in BSE Model 1325 Km.

e) The perturbations appear to bulge with depthl, suggesting that subducted slabs undergo vertical compression and folding? in which case, only the minimum widths of the original slabs can be estimated.

Fig. 4 Overview tectonic sections of the study areas (nomenclature "Almopias, Paikon and Peonian" units after Kockel, 1979).

a) western part of section shows obducted ophiolite, composed of serpentinite, peridotite, basalt, gabbro and radiolarian chert, which was obducted together with tectonic mélange over the Pelagonian carbonate platform (Scherreiks 2000). The Elias formation has been interpreted as a relict of a supra-subduction island arc complex (Scherreiks et al. 2014). Bauxite was deposited during the Callovian (Scherreiks et al. 2016) (Table 1a 5 and 6). The eastern part of section a) shows overthrust, supposed Vardar, Cretaceous platform carbonates and mylonitized ocean floor mélange (devoid of serpentinite). This nappe overlies the post-Eohellenic erosional unconformity of Upper Triassic dolomite (Scherreiks and BouDagher-Fadel 2020a). Section b), shows the Vardar zone between the Guevgueli ophiolite complex and Pelagonian ophiolite near Arnissa. Exposures of Pelagonia-derived ophiolite s. str. occur in the western and central parts of the Almopias zone near Karydia and Lyki/Klisochori; Serpentinite is not found in the units of the Paikon sub-zone (see also Fig. 6).

Fig. 5 Overview geologic map of Skopelos and Alonnisos in the Northern Sporades (based on Matarangas 1992; Kelepertsis 1974 and Scherreiks and BouDagher-Fadel 2020a), The Cretaceous limestone formation of Alonnisos and Skopelos lies tectonically emplaced, together with a sheared mélange of metamorphic ocean-floor basalt and radiolarian chert, on top of the post-Eohellenic erosional unconformity over Pelagonian Upper Jurassic limestone on Alonnisos and Upper Triassic dolomite on Skopelos. It has been postulated that the tectonic emplacement took place during Paleocene time as Pelagonia underthrust the Cretaceous forearc basin of the Vardar volcanic arc (Scherreiks and BouDagher-Fadel 2020a).

Fig. 6 Geologic overview map of the Vardar and adjacent Pelagonian zone (based on Mercier and Vergely 1988 and 1984; Katrivanos et al. 2013; Georgiadis et al. 2016; and own field work). The Pelagonian zone is in an underthrust position relative to the Cretaceous carbonate platform of the Vardar zone (Georgiadis et al. 2016) (B-B´). Imbricated ophiolite and Jurassic limestone are exposed in a window extending from Margarita to Veria. Metamorphosed Pelagonian limestone is exposed in the Gandach antiform of the Paikon sub-zone near Livadia. The tectonic section A-A´is shown in Figure 4b. The formations between the Gandach marble and the Theodoraki limestone is a composite mélange

Fig. 7 Chondrite-normalized REE and ternary discrimination diagrams

a. LREE enriched samples, probably IABs.

b. Flat REE and LREE depleted samples, most likely MORBs (see text).

c. Discrimination diagrams: Vardar-zone data (AFMs are also shown for Evvoia and the Northern Sporades). The AFM from Perfit and others (1980) shows the plots of 1170 IABs (the dashed red line area in the Vardar diagram, encompassing only a few of the Vardar meta-basalts).

Fig. 8 Composite tectono-stratigraphic synopsis:
a) Evvoia and the Northern Sporades were overthrust by the Eohellenic ophiolite which was subsequently deeply eroded and transgressed by ~Cenomanian conglomerates. On the Northern Sporades, the ophiolite and Lower Cretaceous had been removed by erosion before being underthrust (D1-D3) beneath the Vardar-zone sheet during Paleocene time. b) Likewise, the Vardar zone was underthrust by Pelagonia, which carried remnants of Eohellenic ophiolite and possibly Cenomanian orthoconglomerates. c) schematic section through the Vardar ocean between Pelagonia and Serbo-Macedonia indicating the widths (km) of oceanic lithosphere (see seismic tomography). Legend: 1) Cretaceous and Paleocene carbonates. 2) mélange including Triassic radiolarite and basalt, pyroclastic rocks, and carbonate slices. 3) Upper Jurassic (Pelagonian slices) and lower Cretaceous Theodoraki carbonate slices. 4) Pelagonian ophiolite s. str. 5) Pelagonian Jurassic carbonates 6) Pelagonian upper Triassic dolomite 7) Crystalline basement of Pelagonia. D1-D3 deformations (see text)

Fig. 9 Paleogeography and time-laps cartoons
a) The Vardar ocean was situated between two passive margins, continental Adria (including Korab-Pelagonia) and Serbo-Macedonian Europe. Early Middle Jurassic intra-oceanic subduction led to the demise of about 1200 km of Vardar lithosphere and to the obduction of about 200 km of the Eohellenic ophiolite onto eastern Pelagonia. Subsequently, about 1700km of Vardar ocean lithosphere subducted beneath the Paikon (east Vardar) island arc, followed by the crash of eastern Pelagonia with the island arc, and finally (c) to the collision of Pelagonia with Serbo-Macedonia.
b) This time-laps cartoon shows the demise of the Vardar ocean in 7 stages. Pelagonia and Vardar ocean lithosphere move NE toward, relatively autochthonous, Eurasia. Pelagonia and Vardar ocean lithosphere move NE toward, relatively autochthonous, Eurasia. The Vardar ocean slabs are shown as they reach their present position shown in Fig. 3c. It is important to note that the Earth´s curvature has been neglected in the graphic. This creates distortion in the lower mantle making it appear wider than it should be.
Time schedule of subduction
1) The Vardar ocean existed during Late Triassic time verified by radiolarians associated with pillow basalt (Table 1a Carnian-Norian).
2) Intra-oceanic subduction was in progress around Toarcian to Aalenian time (180–170 Ma), based on the metamorphic age of subduction-zone amphibolite mélange (Roddick et al.1979; Spray and Roddick 1980). Relative plate motions, however, had already changed from divergence to convergence, during the Late Triassic, testified by the subsidence of the Rhaetian-Sinemurian peritidal carbonate platform and change to the subtidal platform of Pliensbachian and Toarcian time (Scherreiks et al. 2010) (Table 2a Rhaetian-Pliensbachian). Subduction of slab (x) continued through the Middle Jurassic, verified by late Middle Jurassic radiolarians in ophiolite mélange in Evvoia (Danelian and Robertson 2001; Scherreiks et al. 2014).
3) Platform uplift, erosion and bauxite deposition occurred during the Callovian (Meléndez et al. 2007; Scherreiks et al. 2016), presumably due to the crash of the Eohellenic arc with the Pelagonian platform (Callovian unconformity ibid.), causing upwarping of the carbonate platform. This stress communicated across the east Vardar ocean causing subduction between east Vardar and Serbo-Macedonia.
4) As the Eohellenic ophiolite advanced, the carbonate platform subsided below the CCD during Kimmeridgian-Berriasian time while back arc spreading was taking place in Guevgueli.
5) The final Eohellenic ophiolite emplacement takes place about Valanginian time. The west Vardar slab x breaks off and sinks, the Pelagonian platform rises and deep (post-Eohellenic) erosion of the Eohellenic nappe takes place. The Cretaceous carbonate platform evolves on top of volcanic debris of the forearc basin and accretionary wedge. The east Vardar slab (y) continues to subduct.
6) Pelagonia crashes with the arc, underthrusts the Cretaceous carbonate platform and volcanic arc, and the Guevgueli back arc basin.
7) Pelagonia crashes with Serbo-Macedonia while the Vardar slab breaks off and subsides.

c) The cartoon shows the final episode of Vardar ocean subduction. Pelagonia crashes and underthrusts the arc and the Vardar slab breaks off. Pelagonia collides with Serbo-Macedonia which initiates folding and renewed thrust faulting.

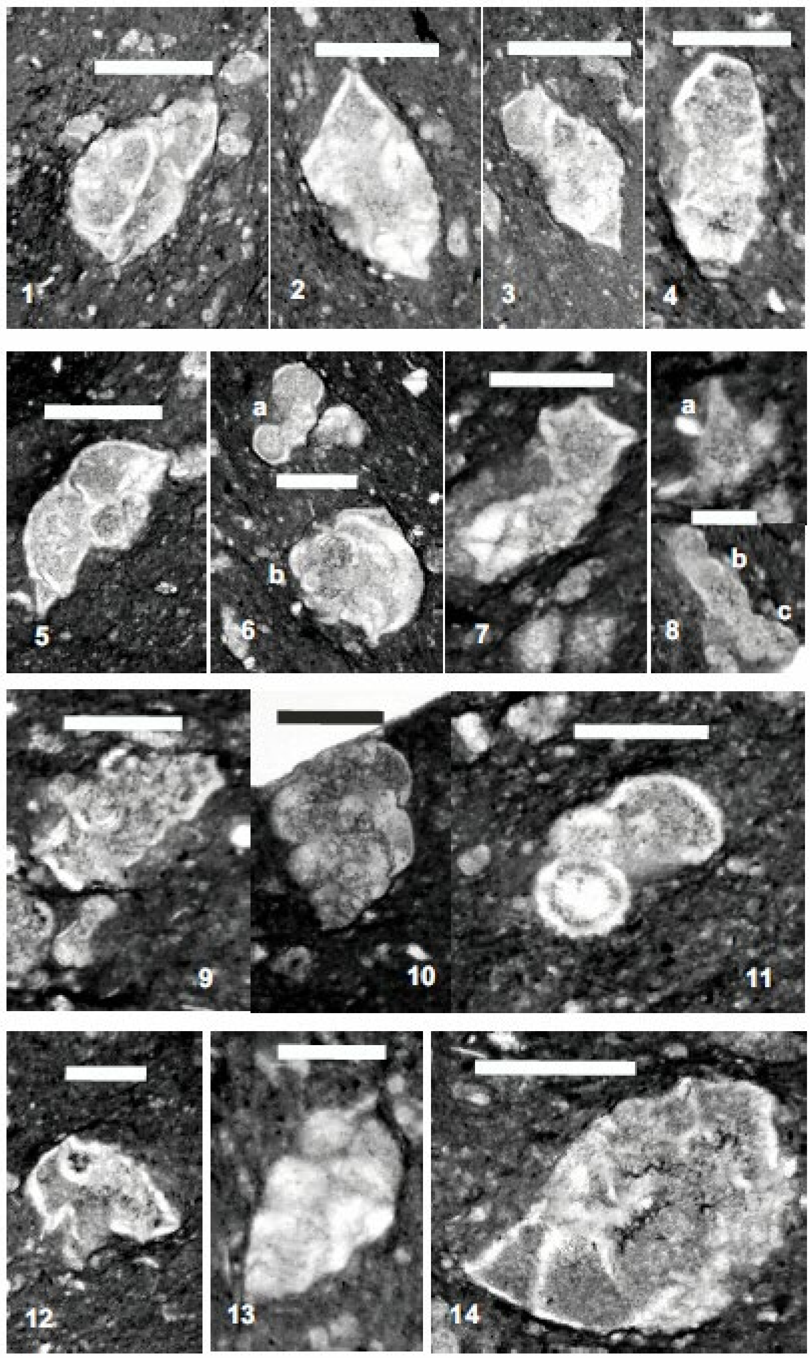

Plate 1

Scale bars: Figs 1 – 14

Fig. 1. *Contusotruncana fornicata* (Plummer).
Fig. 2. *Globotruncanita stuarti* (De Lapparent).
Fig. 3. *Globotruncana arca* (Cushman).
Fig. 4. *Globotruncana linneiana* (d'Orbigny).
Fig. 5. *Radotruncana subspinosa* (Pessagno).
Fig. 6. a) *Rugoglobigerina hexacamerata* Brönnimann, b) *Radotruncana subspinosa* (Pessagno),
Fig. 7. *Globotruncana aegyptiaca* Nakkady.
Fig. 8. a) Schackoina sp., b) *Ventilabrella glabrata* (Cushman), c) *Rugoglobigerina hexacamerata* Brönnimann.
Fig. 9. *Globotruncana lapparenti* Bolli.
Fig. 10. *Heterohelix dentata* (Stenestad).
Fig. 11. *Rugoglobigerina rugosa* (Plummer).
Fig. 12. *Globotruncana rosetta* (Carsey).
Fig. 13. *Heterohelix carinata* (Cushman).
Fig. 14. *Globotruncanita atlantica* (Caron).

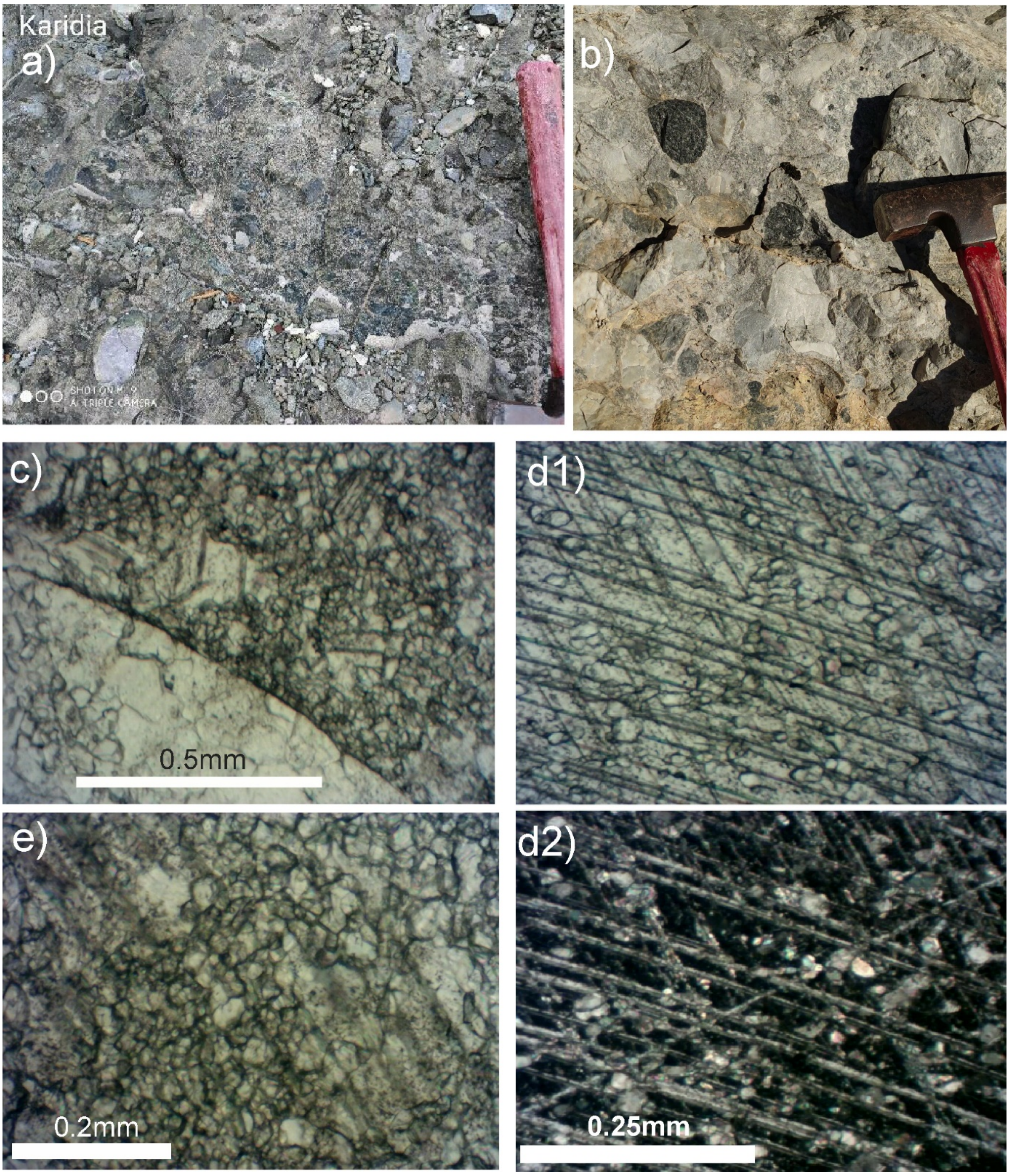

Plate 2a

a. Field photo: breccio-conglomeratic ophiolite mélange in west Almopias, near Karydi

b. Field photo: breccio-conglomeratic carbonate mélange in west Almopias near Nisi

c. Photomicrograph: rounded grain of limestone and adjacent matrix of micro-breccia without cement.

d1 and d2 Photomicrographs: neomorphic calcite (parallel and crossed nicols) in the matrix of 2b, showing palimpsest relic matrix grains and twinning planes.

e-Photomicrograph: matrix of 2b showing initial palimpsest texture of growing neomorphic calcite in the matrix with recognisable twin planes

Table 1a Biostratigraphic data, Evvoia and the Northern Sporades

Table 1a biostratigraphy of Evvoia and Northern Sporades (BouDagher-Fadel 2008; Scherreiks 2000; Scherreiks et al. 2010, 2014; Scherreiks and BouDagher-Fadel 2020a)

Pelagonian carbonate platform **1. Rhaetian-Hettangian: peritidal/subtidal** ? *Aulotortus* sp., ‘‘*Aulotortus friedli*”, *Auloconus permodiscoides, Grillina* sp.‘‘*Vidalina*’’ *martana* **2.Sinemurian-Early Pliensbachian: shallow warm reef environment** *Siphovalvulina colomi, Siphovalvulina gibraltarensis, Duotaxis metula, Lituosepta recoarensis, Riyadhella praeregularis. Lituosepta compressa, Riyadhella praeregularis, Palaeodasycladus mediterraneus, Pseudocyclammina liasica, Lituosepta recoarensis* **3. Aalenian-Bathonian: shallow water environment** *Mesoendothyra croatica* Gusîc´ **4. Middle to Upper Jurassic: shallow water environment** BouDagher-Fadel 2008 *Neokilianina rahonensis*
5. Bathonian-Callovian foraminifera suite: shallow warm reef environment This limestone occurs below the below the bauxite *Pseudomarssonella bipartita*, *Redmondoides medius*, *Andersenolina elongata, Riyadhella* sp. *Ammobaculites* sp., *Trocholina* sp., *Palaeodasycladus* cf. *mediterraneus*, *Pseudopfenderina* sp., *Everticyclammina* sp., *Siphovalvulina* sp., *Riyadhoides* sp. **6. Callovian-Oxfordian foraminifera suite on top of laterite: shallow reef environment** *Chablaisia* sp, *Septatrocholina banneri*, *Andersenolina elongata*, *Andersenolina* sp., *Palaeodasycladus* sp
7. Upper Jurassic shallow patch-reef environment *Protopeneroplis striata*, *Parurgonina caeinensis*, *Thaumatoporella parvovesiculifera, Actinostromaria tokadiensis* **8. Late Berriasian-Early Valanginian: shallow reef environment** *Cladocoropsis mirabilis*, *Zergabriella embergeri*
9. Late Cretaceous transgression in Evvoia, Maastrichtian: outer neritic environment *Plummerita* aff. *hantkeninoides, Idalina* aff *antiqua*, Hippurites sp.,*Planorbulina cretae*: on a rudist clast (Campanian).
Cretaceous carbonate platform of the Northern Sporades **10.1 Albian to Santonian: shallow reef environment** *Nezzazatinella picardi*, *Nezzazata convexa, Dicyclina schlumbergeri* **10.2Late Santonian to Maastrichtian: reef/forereef environment** *Rotorbinella* sp., *Orbitoides* sp., *Lithocodium* sp., *Lithocodium aggregatum*, rudists **10.3 Early Paleocene: shallow reef environment** *Kathina* sp., *Daviesina* sp., *Lockhartia* sp
Radiolarians in Evvoia **11. Ophiolite sheet:** Scherreiks et al. 2014, determined in co-operation with P. O. Baumgartner,Gingins and Schauner (Baumgartner et al. 1995). **11.1 Carnian to Lower Norian:** *Annulotriassocampe* ? sp., *Castrum* ? sp., *Corum* ? sp., *Capnuchosphaera* cf. *crassa Capnuchosphaera* sp. **11.2 Elias complex, Middle to Late Jurassic:** Spongocapsula hooveri, Parvicingula dhimenaensis s.l. Transhuum brevicostatum, Protunuma sp., Sethocapsa sp.
12. Ophiolite mélange (Danelian and Robertson 2001; Gingins and Schauner 2005) **Middle Bathonian to Lower Callovian** *Parvicingula dhimenaensis* ssp., *Mirifusus fragilis* s.l., *Transhsuum maxwelli* gr., *Tricolocapsa plicarum* s.l.

Table 1b West and Central Almopias After Mercier and Vergely 1988 Updated and additional age and palaeoenvironmental determinations (BouDagher-Fadel et al., 2015, 2018a, 2018b)

1. West Almopias **1.1 Late Maastrichtian (Maastr, 2): inner neritic environment** Planktonic foraminifera *Abathomphalus mayaroensis, Globotruncana Stuarti, Contusotruncana contusa, Globotruncana arca* and *Globotruncana linneiana* and the larger benthic foraminifera *Orbitoides medius* **1.2 Santonian-early Campanian: shallow reef/intertidal environments.** The Hippuritidae, Vaccinites atheniensis
2 Kato Grammatiko Pyrgi: Cenomanian (Cen. 1): forereef/inner neritic environment. Planktonic foraminifera *Rotalipora appenninica* and larger benthic foraminifera *Nezzazata simplex*
3. Kerassia Campanian-Maastrichtian (Camp. 3b-Maast 2), : inner to outer neritic environment *Globotruncana arca* [= *G. convexa*], *Globotruncanita* gr. *struarti-stuartiformis*
4 Kerassia – Nisi – Kedronas **4.1 Campanian (3, 77.0-72.1Ma): Inner to outer neritic planktonic foraminifera in micritic wackestone:** *Radotruncana subspinosa*; *Heterohelix dentata*, *H.* spp.; *Globotruncana lapparenti*, *G. aegyptiaca*, *G. ventricosa*, *G. linneiana*, *G. rosetta*, *G. arca;* Contusotruncana *fornicata*; *Ventilabrella glabrata*; *Rugoglobigerina rugosa*, *R. hexacamerata*; *Globotruncanita atlantica*, *Gl. stuarti*, *Gl.* sp.; *Schackoina* sp.; *Globotruncanella* sp.; *Archaeoglobigerina blowi*. **4.2 Aptian (Apt. 1-4a): reefal to inner neritic environment depositional depths of between 10 and 50m.** The presence of the larger benthic foraminifera *Palorbitolina discoidea* Gras (Barremian to Aptian), Palorbitolina lenticularis, indicate Aptian 1-4a age 125-115 Ma (see BouDagher-Fadel and Price, 2019).
5. Kerassia – Kedronas - Kato Grammatiko Campanian-Maastrichtian (Camp.3-Maast): reefal (rudist debris) to reworked in outer neritic Globotruncana *arca*, *Globotruncanita stuarti*, *Globotruncana linneiana* [= *G. tricarinata*] **5.1 Late Santonian (Sant.2): outer neritic** *Globotruncana lapparenti*, *Globotruncana arca* [= *G. convexa*], Marginotruncana coronata, *Sigalia deflaensis* **5.2 Early Santonian (Sant. 1): outer neritic** *Praeglobotruncana turbinata*, *Sigalitruncana sigali*, *Marginotruncana coronata*, *Globotruncana linneiana Globotruncana lapparenti*.
6 Jurassic exposures in the Kerassia-Nisi area (Pelagonian origin) Oxfordian-Early Cretaceous: low energy environment *Stylosmilia* cf. *miehelini*, *Thecosmilia* cf. *langi*, *Cladocoropsis mirabilis*, *Dermosmilia* sp. and *Schizosmilia* cf. *rollieri* indicate a? Late Oxfordian-? Early Kimmeridgian age (in Sharp and Robertson 2006)
7. Central Almopias (**Maragarita and Klissochori** limestones on top of Jurassic mélange) with "conglomeratic" lenses **7.1 Flamouria, (east of Edessa) Early Santonian: outer neritic** *Marginotruncana coronata, Globotruncana arca* [= *G.convexa*, *Marginotruncana marginata*. The shallow water Early Cretaceous. larger benthic foraminifera, *Orbitolina* sp. are reworked into the pelagic assemblages. **7.2 Messimeri (beneath Central Almopias mélange south of Edessa)** *Cladocoropsis* sp. Indicates Late Jurassic age and Pelagonian

Table 1b Biostratigraphic data, west and central Almopias

Table 1c East Almopias and Paikon (after Mercier and Vergely 1984) updated age and environment (BouDagher-Fadel et al.,2015)
1. Nea Zoi **1.1 Cenomanian (Cen. 3): outer neritic environment.** *Rotalipora cushmani* and *Praeglobotruncana stephani* **1.2 Late Santonian-early Campanian (Sant.2-Camp.2): inner to outer neritic** *Globotruncanita elevata*, *Globotruncana convexa*, Globotruncana arca, *Orbitoides media*
?2. Krania-Mavrolakkos Unit. Radiolarian determinations (? P. De Wever & H. YiLing; in Sharp & Robertson 1998; 2006) ages ranging from Callovian to Early Cretaceous?
3. Krania Unit: Mid-Oxfordian to Valanginian Radiolarians reported by Stais (1994).
4. Vryssi Unit and Nea Zoi Unit: basalts are overlain by radiolarite of **Late Triassic** (Stais et al. 1990).
Paikon **5- Theodoraki unit** **5.1 Late Maastrichtian(Maast. 2-3): outer neritic** *Globotruncana linneiana, Contusotruncana contusa*, *Globotruncana arca* 5.2 **Maastrichtian (Maast. 2-3): outer neritic** *Globotruncana arca* [= *G. convexa*], *Globotruncana linneiana* [= *G. tricarinata] Globotruncana calciformis*, *Contusotruncana contusa* indicate late Maastrictian age. **5.3 Early Campanian (Camp 1-2): outer neritic** *Globotruncanita stuartiformis* indicates Campanian Santonian *Marginotruncana marginata* indicates an early Santonian age reworked into early Campanian assemblage. **5.4 Earl Cenomanian (Cen. 1): reef/inner neritic** *Orbitolina* gr. *Concava, Nezzazata* sp., *Cuneolina* sp, *Cycloloculina* sp., *Pseudolituonella* sp. (see BouDagher-Fadel, 2018a)
6. Griva-Khromni mélange (from numerous researchers in Katrivanous et al. 2013). **6.1 Aptian-Early Albian** *Mesorbitolina* sp., *Sabaudia minuta* **6.2 Late Jurassic to Early Cretaceous** *Actinoporella* sp., *Pseudocyclamina* sp., *Cuneolina* sp., *Cladocoropsis mirabilis*, nerineid gastropods

Table 1c Biostratigraphic data, east Almopias and Paikon

Analyte Symbol	SiO2	Al2O3	Fe2O3(T)	MnO	MgO	CaO	Na2O	K2O	TiO2	P2O5	LOI	Total	Sc	Be	V	Ba	Sr	Y	Zr	Cr	Co	Ni	Cu
Unit Symbol	%	%	%	%	%	%	%	%	%	%	%	%	ppm	ppm	ppm	ppm	ppm	ppm	ppm	ppm	ppm	ppm	ppm
Lower Limit	0.01	0.01	0.01	0.001	0.01	0.01	0.01	0.01	0.001	0.01		0.01	1	1	5	2	2	1	2	20	1	20	10
Method Code	FUS-ICP	FUS-ICP	FUS-ICP	FUS-ICP	FUS-ICP	FUS-ICP	FUS-ICP	FUS-ICP	FUS-ICP	FUS-ICP	GRAV	FUS-ICP	FUS-ICP	FUS-ICP	FUS-ICP	FUS-ICP	FUS-ICP	FUS-ICP	FUS-ICP	FUS-MS	FUS-MS	FUS-MS	FUS-MS
14	79.94	4.34	10.05	0.106	0.63	0.36	0.26	0.47	0.387	0.38	3.23	100.2	6	< 1	66	100	135	17	173	90	7	50	20
16	74.42	9.37	2.99	0.049	0.97	3.56	1.77	1.72	0.368	0.08	4.49	99.78	7	1	49	243	152	15	101	160	6	40	10
25	52.87	16.74	11.07	0.166	2.92	7.63	4.97	0.03	0.649	0.02	2.57	99.64	42	< 1	301	8	85	16	26	< 20	33	20	380
26	38.64	4.34	3.05	0.117	2.75	26.13	0.67	0.47	0.370	0.08	22.73	99.34	8	< 1	56	92	463	12	53	400	10	140	10
36	62.02	13.26	6.96	0.175	7.60	0.82	0.01	2.47	0.641	0.13	6.45	100.5	15	2	120	245	9	17	121	250	28	170	20
38	50.18	12.85	11.24	0.157	4.53	6.57	2.47	0.03	2.085	0.24	10.41	100.8	41	< 1	336	36	78	35	129	100	29	40	110
41	54.06	14.10	11.45	0.190	2.85	5.59	4.52	0.46	1.494	0.17	5.97	100.8	35	< 1	303	87	187	29	82	80	38	60	20
44	43.12	13.66	12.54	0.148	6.93	9.31	2.68	0.02	2.235	0.25	9.96	100.9	43	< 1	375	12	117	36	133	90	40	50	20

Analyte Symbol	Zn	Ga	Ge	As	Rb	Nb	Mo	Ag	In	Sn	Sb	Cs	La	Ce	Pr	Nd	Sm	Eu	Gd	Tb	Dy	Ho	Er
Unit Symbol	ppm	ppm	ppm	ppm	ppm	ppm	ppm	ppm	ppm	ppm	ppm	ppm	ppm	ppm	ppm	ppm	ppm	ppm	ppm	ppm	ppm	ppm	ppm
Lower Limit	30	1	1	5	2	1	2	0.5	0.2	1	0.5	0.5	0.1	0.1	0.05	0.1	0.1	0.05	0.1	0.1	0.1	0.1	0.1
14	80	7	1	195	10	6	3	0.6	< 0.2	1	9.5	< 0.5	19.3	29.1	4.14	16.3	3.5	1.65	2.9	0.5	2.8	0.6	1.5
16	30	10	< 1	< 5	62	4	< 2	< 0.5	< 0.2	1	1.4	2.0	15.7	30.6	3.76	14.7	3.1	0.69	2.5	0.4	2.6	0.6	1.6
25	70	15	2	< 5	< 2	< 1	< 2	< 0.5	< 0.2	< 1	0.7	< 0.5	1.5	3.6	0.55	2.9	1.2	0.42	1.8	0.4	2.8	0.7	2.1
26	50	4	< 1	6	15	2	< 2	< 0.5	< 0.2	1	0.5	1.4	6.8	13.9	1.72	6.8	1.6	0.49	1.8	0.3	1.9	0.4	1.1
36	80	15	2	< 5	92	10	< 2	< 0.5	< 0.2	2	< 0.5	3.0	19.3	35.5	4.79	18.5	4.3	1.06	3.8	0.6	4.0	0.8	2.2
38	500	15	< 1	10	< 2	3	< 2	< 0.5	< 0.2	1	0.5	< 0.5	4.1	11.9	2.00	11.5	4.1	0.97	5.8	1.1	7.2	1.5	4.4
41	50	15	1	8	4	< 1	< 2	< 0.5	< 0.2	< 1	1.1	1.6	4.2	12.0	2.00	10.5	3.8	1.29	4.9	0.9	5.6	1.2	3.6
44	100	17	1	< 5	< 2	3	< 2	< 0.5	< 0.2	1	0.7	< 0.5	5.7	15.5	2.66	14.1	4.5	1.63	6.4	1.2	7.6	1.6	4.4

Analyte Symbol	Tm	Yb	Lu	Hf	Ta	W	Tl	Pb	Bi	Th	U
14	0.25	1.6	0.32	3.5	0.4	1	0.3	78	< 0.4	4.7	2.0
16	0.24	1.5	0.26	2.4	0.4	< 1	0.3	11	< 0.4	5.4	1.3
25	0.35	2.4	0.42	0.9	< 0.1	< 1	< 0.1	< 5	< 0.4	0.6	0.3
26	0.16	1.1	0.17	1.1	0.2	< 1	< 0.1	< 5	< 0.4	1.4	0.5
36	0.31	2.1	0.32	2.9	0.7	1	0.4	< 5	< 0.4	8.2	1.6
38	0.66	4.3	0.67	3.3	0.2	1	< 0.1	263	< 0.4	0.3	0.5
41	0.53	3.5	0.55	2.3	< 0.1	2	< 0.1	< 5	< 0.4	0.4	0.4
44	0.64	4.1	0.60	3.2	0.2	< 1	< 0.1	< 5	< 0.4	0.3	0.9

Activation Laboratories Ltd. Report

FUS-ICP, FUS-MS: inductively coupled plasma mass spectrometry

Table 2a major and trace elements for the Vardar zone (Fusion-Inductively Coupled Plasma Mass Spectrometry and Fusion Mass Spectrometry)

	SiO2	Al2O3	Fe2O3(T)	MnO	MgO	CaO	Na2O	K2O	TiO2	P2O5	LOI	Total	Sc	Be	V	Cr	Co	Ni	Cu	Zn	Ga	Ge	As
1 Ev metabas	53.08	13.19	7.30	0.226	10.44	2.80	2.56	1.37	1.147	0.15	6.46	98.74	37	< 1	212	240	35	110	120	110	11	1	< 5
2 Ev serp Nikol	36.86	0.59	8.24	0.089	40.71	0.20	0.01	< 0.01	0.009	< 0.01	11.94	98.66	8	< 1	31	2440	112	2500	< 10	160	< 1	1	< 5
3 Ev perid Mour	42.13	1.08	8.91	0.130	45.25	1.32	0.03	0.01	0.010	< 0.01	-0.20	98.67	12	< 1	47	3040	112	2440	50	120	1	< 1	< 5
4 A1 basalt Agnati	55.42	16.18	9.92	0.111	5.43	1.03	6.11	0.03	0.611	0.04	4.83	99.71	46	< 1	338	< 20	34	20	160	90	15	< 1	18
5 A8 basalt Geor	61.38	16.66	7.44	0.077	4.11	0.32	1.25	2.95	0.815	0.11	4.43	99.55	18	2	137	210	17	110	30	110	21	2	8
6 S5 Bas Paloiki	47.33	15.64	12.26	0.160	7.43	5.78	3.64	0.28	1.959	0.22	5.11	99.81	41	< 1	361	240	42	110	50	120	16	1	< 5
Elias 01	70.94	13.60	5.32	0.121	1.63	0.11	0.42	3.83	0.599	0.06	3.85	100.5	14	2	124	320	16	19	116	70	20	50	70
Elias 02	72.35	11.81	4.72	0.087	1.54	0.14	0.31	3.62	0.499	0.05	3.29	98.4	12	2	106	271	14	12	94	60	18	70	70
Elias 03	53.48	16.03	11.26	0.112	2,55	6.23	6.53	0.13	1.174	0.26	2.61	100.4	38	< 1	333	43	94	18	73	830	31	220	30

	Rb	Sr	Y	Zr	Nb	Mo	Ag	In	Sn	Sb	Cs	Ba	La	Ce	Pr	Nd	Sm	Eu	Gd	Tb	Dy	Ho	Er
1 Ev metabas	31	76	20	80	8	< 2	< 0.5	< 0.2	< 1	< 0.5	1.4	86	10.4	27.4	2.97	12.6	3.3	0.94	3.9	0.7	4.0	0.8	2.4
2 Ev serp Nikol	< 2	2	< 1	< 2	< 1	< 2	< 0.5	< 0.2	< 1	< 0.5	< 0.5	3	< 0.1	< 0.1	< 0.05	< 0.1	< 0.1	< 0.05	< 0.1	< 0.1	< 0.1	< 0.1	< 0.1
3 Ev perid Mour	< 2	< 2	< 1	< 2	< 1	< 2	< 0.5	< 0.2	< 1	< 0.5	< 0.5	3	< 0.1	< 0.1	< 0.05	< 0.1	< 0.1	< 0.05	< 0.1	< 0.1	< 0.1	< 0.1	< 0.1
4 A1 basalt Agnati	< 2	103	17	28	< 1	< 2	< 0.5	< 0.2	< 1	< 0.5	0.6	22	1.9	5.2	0.66	3.2	1.3	0.30	2.0	0.4	2.6	0.6	1.9
5 A8 basalt Geor	130	58	23	162	12	< 2	0.5	< 0.2	3	< 0.5	3.6	462	23.0	49.1	5.54	20.8	4.5	0.97	4.1	0.7	4.3	0.8	2.4
6 S5 Bas Paloiki	7	32	38	153	4	< 2	< 0.5	< 0.2	1	0.5	< 0.5	23	5.4	15.6	2.72	14.3	4.6	1.44	6.7	1.1	7.2	1.5	4.3
Elias 01	70	19	< 1	< 5	137	9	< 2	< 0.5	< 0.2	2	< 0.5	5.5	36.3	78.0	8.04	30.2	5.3	1.04	4.1	0.6	3.9	0.8	2.4
Elias 02	70	14	< 1	< 5	109	8	< 2	< 0.5	< 0.2	2	1.4	4.2	28.1	55.4	6.28	23.3	3.6	0.60	2.1	0.4	2.2	0.5	1.5
Elias 03	100	9	1	6	2	15	< 2	< 0.5	< 0.2	< 1	1.7	< 0.5	9.7	19.1	2.57	11.0	2.6	0.90	2.7	0.5	2.7	0.6	1.7

	Tm	Yb	Lu	Hf	Ta	W	Tl	Pb	Bi	Th	U
1 Ev metabas	0.35	2.2	0.32	1.5	0.8	2	< 0.1	< 5	< 0.4	2.5	0.5
2 Ev serp Nikol	< 0.05	< 0.1	< 0.01	< 0.2	< 0.1	< 1	< 0.1	< 5	< 0.4	< 0.1	< 0.1
3 Ev perid Mour	< 0.05	< 0.1	< 0.01	< 0.2	< 0.1	< 1	< 0.1	7	< 0.4	< 0.1	< 0.1
4 A1 basalt Agnati	0.29	2.0	0.32	0.8	< 0.1	1	< 0.1	< 5	< 0.4	0.7	0.1
5 A8 basalt Geor	0.37	2.3	0.34	4.2	1.0	2	0.4	15	< 0.4	12.2	1.5
6 S5 Bas Paloiki	0.66	4.1	0.61	3.3	0.2	2	< 0.1	< 5	< 0.4	0.3	< 0.1
Elias 01	0.35	2.3	0.35	3.3	0.6	2	0.6	10	< 0.4	11.2	1.8
Elias 02	0.23	1.6	0.26	2.1	0.6	1	0.5	10	< 0.4	8.0	1.3
Elias 03	0.27	1.6	0.29	1.3	0.9	< 1	0.1	< 5	< 0.4	1.4	0.3

Table 2b major and trace elements for Evvoia and the Northern Sporades
(same analytical information as in Table 2a)